NARINGING REVERSES HIV-1 PROTEASE INHIBITORS-ASSOCIATED PANCREATIC β-CELL DYSFUNCTION IN VITRO

By

SANELISIWE NZUZA

207508019

B. Sc. B. Med. Sc. (Hons) (UKZN)

Submitted in fulfilment of the requirements for the degree

of

MASTER OF MEDICAL SCIENCE IN PHARMACOLOGY

Discipline of Pharmaceutical Science, School of Health Sciences, Collage of Health Sciences University of KwaZulu –Natal, Westville campus, Private bag X54001, Durban 4000, South Africa.

Naringin reverses HIV-1 Protease inhibitors-associated Pancreatic beta-cell dysfunction *in vitro*

By

SANELISIWE NZUZA

207508019

B. Sc. B. Med. Sc. (Hons) (UKZN)

Submitted in fulfilment of the requirements for the degree

of

MASTER OF SCIENCE IN PHARMACOLOGY

Discipline of Pharmaceutical Science

Collage of Health Sciences

University of KwaZulu –Natal

As the candidate's supervisor, I have approved this thesis/dissertation for submission

Signed: Name: DR OWIRA PHD Date: 09.04.14

Naringin reverses HIV-1 Protease inhibitors-associated Pancreatic beta-cell dysfunction *in vitro*

By

SANELISIWE NZUZA

207508019

B. Sc. B. Med. Sc. (Hons) (UKZN)

Submitted in fulfilment of the requirements for the degree

of

MASTER OF SCIENCE IN PHARMACOLOGY

Discipline of Pharmaceutical Science

Collage of Health Sciences

University of KwaZulu –Natal

As the candidate's supervisor, I have approved this thesis/dissertation for submission

Signed: S.Nzuza Name: Sanelisiwe Nzuza Date: 07/04/2015

PREFACE

The experimental work described in this dissertation was carried out in the Department of Pharmacology, Discipline of Pharmaceutical Sciences, College of Health Science, University of KwaZulu-Natal, Durban from March 2013 to January 2014 under the supervision of Dr. Owira P.M.O.

The study is an original work of the author and has been submitted in fulfillment of the academic requirements for obtaining a MSc. Degree in Pharmacology. Information from other sources used in this dissertation has been duly acknowledged in the text and reference section.

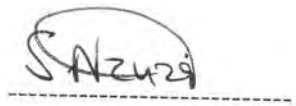

Miss S. Nzuza

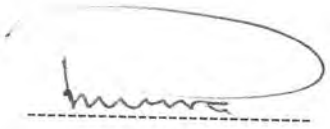

Dr. Owira P.M.O (Supervisor)

DECLARATION – PLAGIARISM

I, Sanelisiwe Nzuza declare that

1. The research reported in this thesis, except where otherwise indicated, is my original research.

2. This thesis has not been submitted for any degree or examination at any other university.

3. This thesis does not contain other persons' data, pictures, graphs or other information, unless specifically acknowledged as being sourced from other persons.

4. This thesis does not contain other persons' writing, unless specifically acknowledged as being sourced from other researchers. Where other written sources have been quoted, then:

a) Their words have been re-written but the general information attributed to them has been referenced.

b) Where their exact have been used, then their writing has been placed in italics and inside quotation marks, and referenced.

5. This thesis does not contain text, graphics or tables copied and pasted from the Internet, unless specifically acknowledged, and the source being detailed in the thesis and in the References sections.

Signed

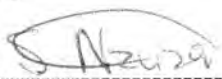

ACKNOWLEDGEMENTS

My parents

Lord said “he has the plans for us, not to harm us but to prosper us. With you everything is possible. Thank you for the words of encouragement.

My beloved mom Thembelihle Sandra Nzuza, Thabisile Nene, Ndumiso Nzuza and Phumlani Nzuza without you I would not be here. Thank you so much for your support, encouragement, motivation and always having a faith in me.

Dr. P. M. O. Owira

Approachable father, I would like to thank you for giving me the greatest opportunity of being the part of your department and experiencing Pharmacology in your vision. Also, the endless love, kindness and advises that you give me throughout my research.

Dr. D. Onyango

I am grateful for all that you have done to assist me in writing my thesis, encouragement, advises and the kindness you showed me through my research.

Ms Kogi Moodley

Many thanks for technical assistance in the Department of Physiology.

Scholarship

The UKZN College of Health Science scholarship, thank you for finding this work.

PRESENTATIONS

S. Nzuza and P. M. O Owira

17th World Congress Pharmacology of Basic and Clinical Pharmacology (July 2014) Cape Town

UKZN College of Health Sciences research symposium (September 2014), Durban, South Africa

"Glibenclamide reverses HIV-1 Protease inhibitors-induced β-cell dysfunction in RIN-5F cells by relieving oxidative stress". Journal: Diabetes, DB15-0048, 13-Jan-2015, Manuscript has been submitted.

LIST OF ABBREVIATIONS

µg/Dl	Micrograms per decilitre
µl	Microliter
µM	Micromolar
•OH	Hydroxyl radical
ADP	Adenosine Diphosphate
AgRP	Agoutigene-Related Protein
AIDS	Acquired immunodeficiency syndrome
AIF	Apoptosis inducing factor
AMPK	Adenosine Monophosphate-activated Protein Kinase
AMPK	Adenosine Monophosphate-activated Protein Kinase
ANOVA	Analysis of variance
Apaf-1	Apoptotic protease activating factor-1
ART	Antiretroviral Therapy
ARVs	Anti-retro viral drugs
ASK-1	Apoptosis Signal-regulating Kinase 1
ATP	Adenosine Triphosphate
Bax	Bcl-2 associated X protein
Bcl-2	B-cell CLL/Lymphoma 2
BHT	Butylated hydroxytoluene
BMI	Body Mass Index
BP	Blood pressure
BSA	Bovine serum albumin
Ca^{2+}	Calcium ion

$CaCl_2$	Calcium chloride
CAD	Caspase activated DNase
cAMP	cyclic Adenosine Monophosphate
CARDs	Caspase recruitment domains
CART	Amphetamine-Regulated Transcript
CCM	Complete culture media
CCR5	Co-receptors Chemokine Receptors (R5-tropic strains)
CH_2	Methylene-carbon
Cm	Centimetre
CO_2	Carbon dioxide
CRABP-1	Cytoplasmic retinoic acid binding protein type 1
CXCR4	C-X-C chemokine receptor type 4
CYP3A4	Cytochrome P450 3A4
CYP450	Cytochrome P450
DEDs	Death Effector Domains
DMSO	Dimethyl sulphoxide
DNA	Deoxyribonucleic Acid
Ds	Double stranded
EDTA	Ethylenediaminetetraacetic acid
eIF4F	Eukaryotic translation initiation factor 4F
eIF4G	Eukaryotic translation initiation factor 4 gamma
ELISA	Enzyme-linked immunosorbent assay
ERKs	Extracellular signal-related kinases
ETC	Electron transport chain
$FADH_2$	Flavin Adenine Dinucleotide

FBS	Fetal bovine serum
Fe^{2+}	Ferrous
g	Gravitational force
GLUT-4	Glucose transporter isoform 4
GPx	Glutathione peroxidise
GR	Glutathione reductase
GSH	Glutathione
GSSG	Glutathione disulphide
GST	Glutathione-S-transferase
H	Hour(s)
H	Hydrogen
H_2O	Water
H_2O_2	Hydrogen peroxide
H_3PO_4	Phosphoric acid
HAART	Highly Active Anti-Retroviral Therapy
HCl	Hydrochloric acid
HIV	Human immunodeficiency virus
IAP	Inhibitor of apoptosis protein
IL-6	Interleukin 6
IRS	Insulin Receptor Substrate
JAK/STAT3	Janus kinase signal transducer and activator of transcription 3
JNK	c-Jun N-terminal Kinases
K_{ATP}	ATP-sensitive potassium
KCl	Potassium chloride
KRBB	Krebs Ringer Bicarbonate Buffer

LRP	LDL receptor-related protein
MAPK	Mitogen-activated Protein Kinase
MDA	Malondialdehyde
mg/dL	Milligrams per decilitre
Mg^{2+}	Magnesium
$MgSO_4$	Magnesium sulphate
Min	Minute(s)
Ml	Millilitre
mM	Millimolar
Mn^{2+}	Manganese
MnSOD	Manganese Superoxide DismutasE
NaCl	Sodium Chloride
NADH	Nicotinamide Adenine Dinucleotide
NaH_2PO_4	Monosodium phosphate
$NaHCO_3$	Sodium bicarbonate
NCEP ATP III	National Cholesterol Education Program Adult Treatment Panel
NNRTIs	Non-Nucleoside Reverse Transcriptase Inhibitors
NPY	Neuropeptide Y
NRTIs	Nucleoside Reverse Transcriptase Inhibitors
O_2	Oxygen
$O_2^{\bullet-}$	Superoxide
P	Statistical probability
PARP-1	Poly (ADP-ribose) polymerase-1
PBS	Phosphate buffer saline
PI3K	Phosphatidylinositol 3-kinase

PIs	Protein Inhibitors
POMC	Pro-opiomelanocortin
PPAR-γ	Peroxisomal Proliferator–Activated Receptor γ
PUFA	Polyunsaturated fatty acid
RA	Retinoic Acid
RFU	Relative Fluorescence Units
RLU	Relative light unit
RNA	Ribonucleic acid
ROS	Reactive oxygen species
Rpm	Revolutions per minute
RT	Room temperature
RXR	Retinoic X receptor
RXR	Retinoic X receptor
SEM	Standard error of the mean
Smac/DIABLO	Second mitochondria-derived activator of caspases/DIABLO
SNPs	Single Nucleotide Polymorphisms
SOC3	Suppressor of Cytokine signaling 3
SOD	Superoxide dismutase
SREBP-1c	Sterol Regulatory Element Binding Protein-1c
ssRNA	single-stranded RNA
SUR1	Sulfonylurea receptor 1
TBA	Thiobarbituric acid
TBARS	Thiobarbituric acid reactive substances
TCA	Tricarboxylic Acid
TMB	Tetramethylbenzidine

TNF	Tumor Necrosis Factor
TNF-α	Tumor Necrosis Factor-alpha
UCP2	Uncoupling Protein 2
UNAIDS	United Nations Programme on HIV/AIDS
VLDL	Very Low Density Lipoprotein
WHO	World Health Organisation
WST	Water-Solution tretrazolium

LIST OF FIGURES

Chapter one

Chapter two

Chapter three

LIST OF TABLES

ABSTRACT

Introduction: Chronic exposure to HIV-1 Protease Inhibitors (PIs) has been associated with pancreatic β-cell dysfunction and impairment of insulin secretion. PIs have been suggested to induce β-cell dysfunction through increasing oxidative stress leading to impaired insulin secretion. The study investigated whether naringin, a naturally occurring antioxidant, could reverse PIs-induced β-cell dysfunction by reducing oxidative stress.

Methods: The RIN-5F cells were cultured in RPM1-1640 medium, allowed to grow to 80% confluence, exposed to different concentrations of PIs [nelfinavir (1-10 μM), saqanavir (1-10 μM) and atazanavir (5-20 μM)] in the presence of 11 mM glucose for 24 hr then subjected to insulin ELISA assay to assess dose-dependent suppression of insulin of secretion by PIs. To determine glucose-induced insulin secretion, the cells were exposed to nelfinavir (10 μM), saquinavir (10 μM), atazanavir (20 μM) 24 hr with or without glibenclamide (10 μM) in the presence of varying glucose concentrations (11-25 mM) then harvested and subjected to biochemical assays for the measurement of insulin levels, lipid peroxidation, ATP generation, Glutathione levels (GSH), Superoxide dismutase (SOD) and caspase-3 and -9 activities.

Cells were further exposed to naringin (0-50 μM) in the presence of 11 mM glucose for 24 hr then subjected to insulin ELISA for insulin secretion determination. To investigate the role of PIs relative to naringin on RIN-5F cells, the cells were exposed to nelfinavir (10 μM), saquinavir (10 μM) and atazanavir (20 μM) with or without naringin (10 μM) also in the presence of 11 mM for 24 hr and similarly subjected to biochemical assays.

Results: Linear regression analysis showed significant decrease in insulin levels in response to nelfinavir, saqunavir and atazanavir (r^2= 0.86, 0.76, 0.95, respectively) in a dose-dependent manner. PIs significantly ($p < 0.05$) reduced insulin secretion and ATP production, increased lipid peroxidation, SOD and caspase-3 and -9 activities and also reduced GSH in a glucose-

dependent manner. These effects were reversed by glibenclamide. Naringin (0-50 μM) caused dose-dependent increased in insulin secretion and also reduced lipid peroxidation, SOD, caspase-3 and -9 activities, increased GSH and ATP levels in cells that were exposed to PIs.

Conclusion: PIs induced β-cell dysfunction and impairment of insulin secretion by increasing oxidative stress and ATP depletion. Naringin ameliorated PIs-induced impairment of β-cell dysfunction by reducing oxidative stress.

TABLE OF CONTENTS

CHAPTER ONE

1. Introduction

1.1. HIV epidemiology

Human immunodeficiency virus-1 (HIV-1) remains a global health problem even after 25 years since the epidemic began (Maartens et al., 2014). According to the current statistics, approximately 35.3 million people are living with HIV and 1.6 million died of human immunodeficiency virus/acquired immunodeficiency syndrome (HIV/AIDS)-related illnesses globally (UNAIDS., 2013). HIV prevalence appears to be higher in individuals residing in low income countries (95%) compared to individuals residing in high income countries (UNAIDS., 2013). Sub-Saharan Africa has the most serious HIV-1 epidemic worldwide with approximately 25 million individuals living with HIV, which accounts for 70% of the worldwide total population (Beyrer and Abdool Karim, 2013). In these countries, HIV-1 contagion has remarkable consequences on civilization, affecting life expectancy occupants, decelerating economic growth and increasing poverty (UNAIDS., 2013)

South Africa has a highest incidence of HIV globally, with 5.6 million individuals currently living with HIV-1 (Bekker et al., 2014). According to UNAIDS, the total number of South Africans infected with HIV has increased from 4.1 million in 2001 to 5.7 million in 2010 (Bekker et al., 2014). The HIV-1 prevalence appears to be higher in females (45%) between the ages of 15-49 years, and 20% being children under the age of 15 years (Bekker et al., 2014). According to World Health Organisation, this is partly due to the fact that most individuals are ignorant of their status (Bekker et al., 2014; Castilla et al., 2005).

1.2 HIV treatment

The introduction of antiretroviral drugs (ARVs) in 1996 has greatly improved the natural course of the disease in the affected individuals (Anuurad et al., 2010). They reduce viral replication, increasing CD4+ count, thus decreasing the risk of contracting opportunistic infections that frequently lead to death (Kis et al., 2010; Rudich et al., 2001). There are six different classes of ARVs permitted by World Health Organisation (Apostolova et al., 2011; Dau and Holodniy, 2008). They include 1) entry inhibitors which bind to the host CCR5 receptors, therefore preventing interaction of viral gp120 and host CCR5 which is necessary for the entry into the host cell; 2) Fusion inhibitors which prevent entry of viral nucleic acid into the host CD4 cell (Apostolova et al., 2011; Dau and Holodniy, 2008; Loonam and Mullen, 2012); 3) Nucleotide Reverse Transcriptase Inhibitors (NRTIs) which are false nucleoside analogues, which act as substrates incorporated into the active site of HIV reverse transcriptase leading to termination of chain elongation (Apostolova et al., 2011; Dau and Holodniy, 2008; Kis et al., 2010); 4) Non-nucleosides Reverse Transcriptase Inhibitors (NNRTIs) that bind allosterically to a hydrophobic pocket situated at 10 amino acid residues away from catalytic site of the enzyme (Apostolova et al., 2011; Dau and Holodniy, 2008; Loonam and Mullen, 2012). Therefore, the binding of NNRTI induces conformation changes at Tyr-181 and Tyr-188 residues, affecting active site of reverse transcriptase and thereby preventing HIV-1 replication; 5) Integrase Inhibitors (IIs) block the integration of viral cDNA to the host genome (Dau and Holodniy, 2008; Kis et al., 2010). It binds to the active site of Mg^{2+} within HIV-1 integrase, thus blocking active site from binding to target DNA strand; 6) protease inhibitors (PIs) bind to the substrate side of the enzyme, imitating tetrahedral intermediates of its substrate (Dau and Holodniy, 2008; Loonam and Mullen, 2012). This leads to inhibition of HIV-1 proteases and subsequently production of immature proteins and non-infectious virons (Apostolova et al., 2011; Kis et al., 2010; Loonam and Mullen, 2012).

Table 1: Antiretroviral drugs for treatment of HIV infection (Dau and Holodniy, 2008).

Drugs class	**Available Antiretroviral Agents**
Entry inhibitor	Maraviroc (MAC)
Fusion inhibitor	Enfuvirtide (T-20)
Integrase inhibitor	Raltegravir (RAL)
Nucleoside reverse transcriptase inhibitor (NRTI)	Abacavir (ABC) Didanosine (ddI) Emtricitabine (FTC) Lamivudine (3TC) Stavudine (d4T) Tenofovir (TDF) Zidovudine (AZT or ZDV)
Non-nucleoside reverse transcriptase inhibitor (NNRTI)	Abacavir (ABC) Didanosine (ddI) Emtricitabine (FTC) Lamivudine (3TC) Stavudine (d4T) Tenofovir (TDF) Zidovudine (AZT or ZDV)
Protease inhibitor (PI)	Atazanavir (ATV) Darunavir (DRV) Fosamprenavir (fAPV) Indinavir (IDV) Nelfinavir (NFV) Ritonavir (RTV) Saquinavir (SQV) Tipranavir (TPV)

The current guidelines for HIV management constitute Highly Active Antiretroviral Therapy (HAART) include the use of three different classes of antiretroviral drugs; 2 NRTIs and 1 NNRTIs or 1 PIs (Feeney and Mallon, 2011; Loonam and Mullen, 2012). The use of the fixed

dose antiretroviral therapy has also been introduced (April 2013) by the Department of Health in South Africa in order to improve compliance of those being treated with the antiretroviral agents (Clinicians Society, 2013; Gandhi and Gandhi, 2014).

While improving the clinical course of HIV positive patients, it has become apparent that the long-term use of HAART especially those containing PIs in the management of HIV often results in the development of symptoms of metabolic syndrome such as lipodystrophy, dyslipidemia, insulin resistance (Heath et al., 2002; Souza et al., 2013; Vu et al., 2013; Woerle et al., 2003). Approximately 60% of HIV patients treated with PI-containing therapy developed either glucose intolerance or insulin resistance and 83% developed lipodystrophy (James et al., 2002; Rudich et al., 2001; Saves et al., 2002; Woerle et al., 2003).

Metabolic syndrome has been documented as a multifactorial risk factor of cardiovascular disorder by U.S. National Cholesterol Education Program Adult Treatment Panel (NCEP ATP) III report and type 2 diabetes (Barbaro, 2006; Cahn et al., 2010). The NCEP ATP III identifies metabolic syndrome at parametric risk factors viz:- (a) abdominal obesity, assessed as waist circumference > 102 cm (males) and 88 cm (females); (b) fasting glucose > 100 ng/dl (c) blood pressure (BP) ≥ 130/85 mmHg; (d) HDL-cholesterol < 40 mg/dL (males) and < 50 mg/dL (females) (e) triglycerides > 150 mg/dl and insulin resistance (Alberti et al., 2005; Samaras et al., 2009). Early diagnosis could prevent development of type 2 and cardiovascular diseases (Alberti et al., 2005; Gayoso-Diz et al., 2013; Samaras et al., 2007).

The risk factors of metabolic syndrome include genetic factors such as polymorphism or mutation of peroxisome-proliferator-activated receptor gamma 2 gene, chromosome 10p (Rankinen et al., 2006), melanocortin-4 receptor gene, beta-adrenergic receptors, Tumor Necrosis Factor (TNF), Neuropeptide Y (NPY) (Yeo et al., 1998), Pro-opiomelanocortin

(POMC) (Krude et al., 1998), leptin and leptin receptor (Montague et al., 1997), obesity, physical inactivity and smoking. These risk factors have been suggested to induce insulin resistance, hyperinsulinemia, endothelial dysfunction, inflammation cardiovascular disorders (Waters and Nelson, 2007)

1.3 Protease Inhibitors and Metabolic Syndrome

1.3.1 Lipodystrophy

Lipodystrophy includes loss of peripheral subcutaneous fat (lipoatrophy) and central fat accumulation (lipohypertrophy), which may occur separately or exist in both forms in a single patient (Guaraldi et al., 2005; Mencarelli et al., 2012; Vu et al., 2013). Lipoatrophy occurs mainly on the face, arms, buttocks and legs whereas lipohypertrophy occurs at the back of the neck or suprapubic region ("buffalo hump"), abdominal adiposity and mammary hypertrophy (Guaraldi et al., 2005; Palios et al., 2012; Waters and Nelson, 2007). The incidence of lipohypertrophy has varied from 6% (men) to 93% (women) in HAART-treated patients (Bonnet, 2010).

Several mechanisms by which PIs contribute to lipodystrophy have been proposed (Carper et al., 2008; Singhania and Kotler, 2011). PIs have been shown to suppress adipocyte differentiation by inhibiting cytoplasmic retinoic acid binding protein type 1 (CRABP-1) and PPAR-γ (Bonnet, 2010; Tsiodras et al., 2010), which play a role in the differentiation of preadipocyte into mature adipocytes (Tsiodras et al., 2010). The catalytic site of HIV-protease shares approximately 60% homology region within CRABP-1 region (Carr, 2000; Carr and Cooper, 2000). Under normal circumstances, CRABP-1 binds to intracellular retinoic acid (RA) and presents it to cytochrome P450 3A, which in turn converts to cis-9-retinoic, a major ligand of the retinoic X receptor (RXR) (Dau and Holodniy, 2008; James et al., 2002). Then,

the heterodimerization of RXR with PPAR-γ significantly enhances the binding affinity of cis-9-retinoic to RXR (Carr et al., 1998; Dau and Holodniy, 2008; James et al., 2002). The complex cis-9-RA-RXR-PPAR-γ, thus enhances the transcription of genes that prevent adipocytes from apoptosis and increase adipocytes differentiation (Carr, 2000; Carr et al., 1998; Dau and Holodniy, 2008). Carr et al (1998) suggested that PIs may obstruct CRABP-1, therefore preventing CRABP-1 mediated cis-9-RA and decrease stimulation of RXR: PPAR-γ complex. This in turn inhibits peripheral adipocyte differentiation, stimulate adipocytes apoptosis and sequent hyperlipidaemia (Carr, 2000; Dau and Holodniy, 2008). PIs have also been suggested to inhibit cytochrome P450 3A (Aberg, 2009; Carr, 2000), thus reducing conversion of RA to cis-9-retinoic, which also contributes to the impairment of peripheral adipocytes differentiation and hyperlipidemia (Carr, 2000; Dau and Holodniy, 2008; Singhania and Kotler, 2011). The Pls have also been suggested to decrease expression of PPAR-γ (Dau and Holodniy, 2008), an adipocyte receptor that regulates peripheral adipocyte differentiation and apoptosis, and sequent hyperlipidaemia (Carr et al., 1998; Dau and Holodniy, 2008).

Moreover, PIs have been suggested to inhibit low density lipoprotein-receptor-related protein (LRP) by binding to it homologues sequence of HIV protease catalytic region (Carr and Cooper, 2000; Carr et al., 1998; Leow et al., 2003). Low density lipoprotein-receptor-related protein is a part of the low density lipoprotein (LDL) receptor group, responsible for taking up chylomicron remnants enrich with triglycerides to the liver (Hui, 2003). Therefore, it inhibition by PIs reduced clearance of chylomicrons in the liver and breakdown of triglycerides, subsequently leading to hyperlipidaemia (Carr et al., 1998; Leow et al., 2003). PIs also appeared to inhibit proteasome-mediated breakdown of apolipoprotein B (ApoB) also by binding to homologous site of HIV-1 protease (Estrada and Portilla, 2011; Leow et al., 2003; Singhania and Kotler, 2011). ApoB is the primary protein part of triglyceride and cholesterol-rich plasma lipoproteins, serve as enzyme cofactors, ligands of cell-surface receptors as the

lipids are taken up by tissues (Hui, 2003). Therefore, the inhibition of proteasomal degradation resulting in overproduction and circulation of triglyceride-rich lipoproteins (Estrada and Portilla, 2011; Leow et al., 2003; Singhania and Kotler, 2011). Recent data from cross-sectional studies have validated that compared to healthy individuals, PI-treated patients have an increased secretion and reduced clearance of VLDL particles, increased synthesis and reduced catabolism of apoB, elevated levels of pro-atherogenic residue lipoproteins and reduced activity of lipoproteins lipase (Anuurad et al., 2010; Estrada and Portilla, 2011).

Pls have also been shown to affect lipoprotein production regulated by sterol regulatory element binding proteins (SREBPs) (Carper et al., 2008; Hui, 2003), transcriptional regulators of genes involved in lipids and glucose metabolism (Estrada and Portilla, 2011). The SREBPs are lipid sensors, triggered by the decreased levels of intracellular lipid (Estrada and Portilla, 2011; Singhania and Kotler, 2011). They are then transported from the endothelium reticulum to the nucleus where they increase expression of genes involved in triglyceride, fatty acids, cholesterol synthesis and transportation (Estrada and Portilla, 2011; Singhania and Kotler, 2011). Thereafter, they are degraded by the proteasomes within the nucleus (Estrada and Portilla, 2011; Singhania and Kotler, 2011). The PIs especially indinavir and ritonavir have been suggested to activate SREBP-1 and SREBP-2 in the liver (Estrada and Portilla, 2011). The accumulation of these regulators in the hepatocytes promotes cholesterol and fatty acid synthesis, and decrease triglyceride storage (Estrada and Portilla, 2011; Singhania and Kotler, 2011). This is followed by the increased circulation of lipids and triggering lipodystrophy and insulin resistance in the tissues (Estrada and Portilla, 2011; Singhania and Kotler, 2011).

1.3.2 Protease Inhibitors and insulin resistance

Several mechanisms have been suggested by which PIs induce insulin resistance and diabetes. These include suppression of glucose transporters isoform 4 (GLUT4, SLC2A4) function (Carper et al., 2008; Singhania and Kotler, 2011) and alteration of secretion of adipokines such as TNF-α, Interlukin- 6 (IL-6), adiponectin, leptin ad resistin (Anuurad et al., 2010; Tsiodras et al., 2010). Elevated serum levels of cytokines TNF-α (Waters and Nelson, 2007) and IL-6 have been observed in adipose tissue of PI-induced insulin resistance (Crawford et al., 2013). Mynarcik et al., (2000) demonstrated the high levels of sTNFR-2 (soluble type 2 tumor necrosis factor-α) receptors in lipodystrophic patients, reflecting stimulation of TNF-α pathway via TNF-α, a well-known insulin resistance inducer (Flint et al., 2009; Tsiodras et al., 2010). It has been suggested that TNF-α induces insulin resistance through decreasing insulin receptor kinase activity, thus prompting apoptosis and lipolysis by suppressing expression of insulin receptor kinase substrate (IRS)-1 and GLUT-4 (Domingo et al., 2005; Loonam and Mullen, 2012). These alterations have been proposed to occur via diminishing of insulin signalling; reduction of anti-lipolytic function of insulin (Rudich et al., 2005); suppression of inhibitory G protein-coupled receptors, which result in increased cyclic AMP-levels (Zhang et al., 2002); reduced activity of lipoprotein lipase and suppression of lipin, a lipid droplet-associated protein that plays a role in protecting adipocyte from hydrolytic action of lipase (Domingo et al., 2005; Loonam and Mullen, 2012).

Interleukin-6 is a cytokine that is also secreted by immune cells, endothelial cells and fibroblasts in response to inflammation, destruction of immune cells and tissue damage (Bastard et al., 2002; MacDermott, 1996). In adipocytes, IL-6 acts as suppressor of insulin signaling in hepatocytes (Bastard et al., 2002; Qatanani and Lazar, 2007). It has been suggested to down-regulate insulin receptor substrate (IRS) and up-regulate suppressors of cytokine signaling 3 (SOC3; a distinguished negative controller of insulin signaling) (Rieusset et al.,

2004; Wallenius et al., 2002). Due to these actions, it therefore prevents insulin from promoting the absorption of fatty acids and glycerol by adipocytes where they are stored as triglycerides (Petersen et al., 2005; Stith and Luo, 1994).

Low levels of adiponectin have been experimentally demonstrated in individuals with acquired lipodystrophy and insulin resistance (Leung and Glesby, 2011; Loonam and Mullen, 2012). Adiponectin is known as an effective insulin sensitizer (Leung and Glesby, 2011). It has been suggested that adiponectin induces insulin sensitivity by activating adenosine monophosphate-activated protein kinase (AMPK) both in skeletal muscle and the liver, which therefore endorses fatty acid oxidation and decreases production of glucose in the liver (Fruebis et al., 2001; Leung and Glesby, 2011; Qatanani and Lazar, 2007). According to Chaparro et al., (2005), PIs could be lowering the concentrations of adiponectin by down-regulating the expression of SREB-1/PPAR-γ which mediates it transcription; therefore decreasing insulin sensitivity, subsequently leading to insulin resistance.

Even though PIs are reported not to have an effect on serum leptin expression; the effect on leptin in HAART-treated individual depends on the body's stability between fat loss and increased gene expression (Remedi and Nichols, 2009; Tsiodras et al., 2010). Leptin is a peptide hormone produced mainly by adipocytes of white adipose tissue (Bastard et al., 2002; Remedi and Nichols, 2009). Its secretion is positively related to fat mass, with increasing secretion as fat deposal increases (Bastard et al., 2002; Frederich et al., 1995; Friedman, 2009). This peptide acts to decrease food intake and to enhance sympathetic nervous system activity (Frederich et al., 1995; Friedman, 2009). It is transported across the blood-brain barrier and attaches to specific receptor (Ob-Rb) on appetite-regulating neurons and arcuate nucleus of hypothalamus, therefore suppressing appetite and increase energy expenditure respectively (Ashcroft and Rorsman, 2013; Friedman, 2009). In the arcuate nucleus, leptin induces production of POMC and CART to decrease food intake and NPY and AgRP to stimulate food

consumption (Ashcroft and Rorsman, 2013; Shiozaki et al., 2002). In lipoatrophic patients, reduced serum leptin level has been due to the fact that it is mainly found circulating in subcutaneous fat (Tsiodras et al., 2010). However, in lipohypertrophic patients, higher leptin concentrations have been reported (Tsiodras et al., 2010). The role of resistin (a peptide hormone that is known to affect glucose metabolism by antagonizing insulin action) on PI-inducing lipodystrophy and metabolic abnormalities is not known yet. Despite this, resistin is thought to act synergistically with PIs to inhibit adipocyte differentiation and enhance lipoatrophy (Tsiodras et al., 2010). Other adipokines that have been reported in lipodystrophic subjects include retinol binding protein- 4, visfatin, acylation stimulating protein, omentin and vaspin (Remedi and Nichols, 2009; Tsiodras et al., 2010).

Glucose transporter isoform 4 is predominantly expressed in skeletal muscle and adipose tissue, and is responsible for glucose uptake into the cells (Hruz et al., 2001). In general, insulin binds to adipocyte insulin receptor and induces translocation of GLUT 4 from the cytoplasm to the plasma membrane, thereby facilitating adipocyte glucose uptake and triglycerides synthesis (Hruz et al., 2001; James et al., 1989). The PIs inhibit GLUT 4 action (Carper et al., 2008; Koster et al., 2003; Singhania and Kotler, 2011); reduce glucose uptake and triglyceride synthesis (Carper et al., 2008; Flint et al., 2009; Singhania and Kotler, 2011). The reduced glucose uptake increases glucose concentration in plasma leading to hyperglycaemia (Flint et al., 2009; Koster et al., 2003; Leow et al., 2003). The reduction of triglyceride synthesis contributes to adipocytes shrinkage and lipoatrophy (Flint et al., 2009; James et al., 2002). Flint et al., (2009) reported that the exposure of skeletal muscle, 3T3-L1 adipocytes and primary adipocytes to PIs (indinavir, ritonavir and APV), results in suppression of GLUT 4 transport function but with no effects on GLUT 4 translocation or insulin signalling cascade. However, previous studies evaluated the relationship between PI structure and the suppression of GLUT-4-related glucose uptake (Heath et al., 2002). Researchers have found that all

available PIs have analogous phenylalanine-like core structure bounded by hydrophobic moieties, and that the peptide suppresses GLUT4 (Heath et al., 2002). All have highly enclosed aromatic core peptide bound by hydrophobic moieties similar to the structure enclosed by PIs (Heath et al., 2002). Furthermore, PIs have been postulated to induce β-cell dysfunction and are linked to impaired glucose stimulated-insulin secretion in pancreatic β-cells (Chandra et al., 2009; Koster et al., 2003; Schutt et al., 2004)

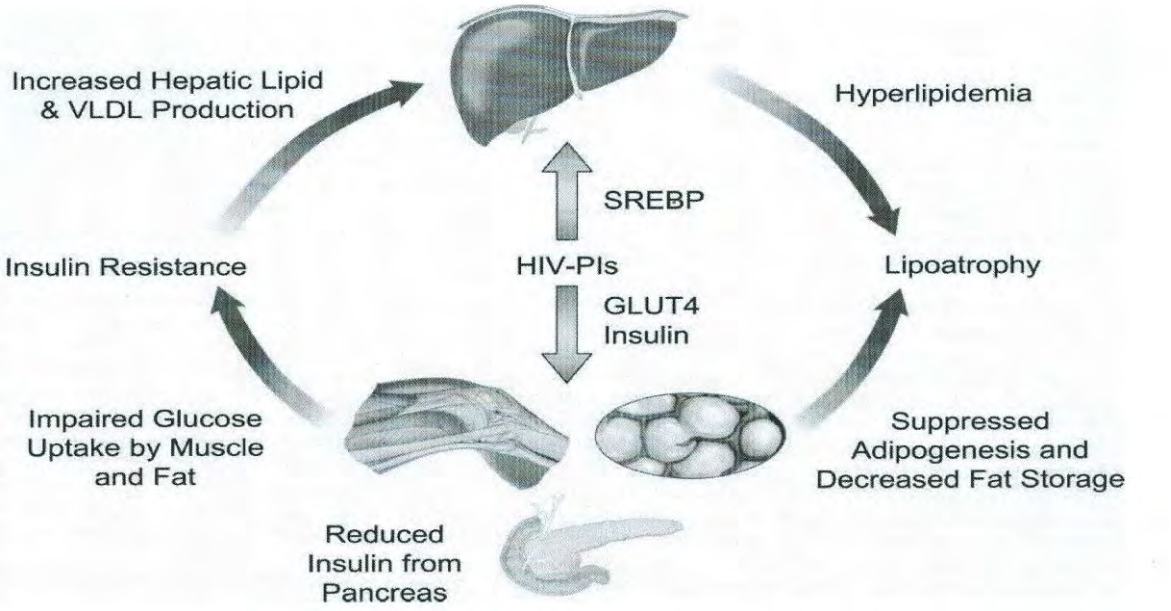

Figure 1: Illustration of Protease inhibitors- mediated metabolic syndrome (Flint et al., 2009). Copyright permission for reproduction was granted from the author.

However, there is limited information involving PIs exposure to β-cells. Current studies have reported that chronic exposure to PIs is associated with pancreatic β-cell dysfunction and impairment of insulin secretion (Koster et al., 2003; Schutt et al., 2004). Chandra et al., (2009) demonstrated that acute treatment with PIs (nelfinavir, saqunavir, atazanavir) significantly inhibited insulin secretion in rat insulinoma cell line (INS-1). Similarly, Koster et al., (2003)

demonstrated that long-term and acute treatment with PIs (ritonavir, indinavir, saquanavir, nelfinavir and atazanavir) significantly inhibited insulin secretion in mouse insulinoma cell line (MINS). The mechanisms by which PIs diminish insulin secretion remain elusive (Chandra et al., 2009). However, it has been suggested that PI-mediated β-cell dysfunction is associated with an increased oxidative stress and decrease ATP synthesis by electron transport chain (Chandra et al., 2009).

1.4 Oxidative stress and Insulin secretion by pancreatic β-cells

Oxidative stress is defined as an imbalance between the production of ROS and the cellular antioxidant enzymes [superoxide dismutase (SOD), glutathione peroxidase (GPx) and glutathione (GSH)] (Ahmadi et al., 2013). It occurs when the production of ROS overpowers the detoxification and scavenging ability of antioxidant defenses resulting in cellular damage (Ahmadi et al., 2013). Electron flow across the mitochondrial electron transport chain is carried out by four inner membrane-associated complexes (I-IV), cytochrome C and carrier coenzyme Q (Murphy, 2009). The electron transport chain (ETC) produces ROS [superoxide ($\bullet O_2$), hydrogen peroxide (H_2O_2), and hydroxyl radical ($\bullet OH$)] normally during cellular respiration (Kanno et al., 2003; Murphy, 2009). Superoxide is produced continuously by ETC in small amounts, this reaction occurs at ETC complexes I (NADH dehydrogenase) and III (ubisemiquinone) (Murphy, 2009; Turrens, 2003). Superoxide is then scavenged by the mitochondrial enzyme manganese superoxide dismutase (MnSOD) to produce hydrogen peroxide (Kanno et al., 2003; Kim et al., 2009). Hydrogen peroxide is converted to water molecule by GPx or catalase in the present of reduced GSH as a coenzyme, thus entirely detoxifying ROS (Murphy, 2009; Turrens, 2003). Excessive generation of H_2O_2 results in production of a highly reactive OH• through Fenton reaction in the presence of ferrous (Fe^{2+}) and through Haber-Weiss reaction (Halliwell and Chirico, 1993; Kanno et al., 2003). If there is no rapid detoxification of ROS, the ROS turns to oxidize mitochondrial components

endorsing proteins crosslinking, DNA fragmentation, phospholipids peroxidation and by triggering a chains of stress pathways (Sreelatha and Padma, 2011).

Oxidative phosphorylation in the inner mitochondrial membrane plays a key role in glucose-induced insulin secretion from the pancreatic β-cells (Chandra et al., 2009; Lowell and Shulman, 2005). Glucose equilibrates through the cell membrane and phosphorylated by glucokinase which defines the rate of glycolysis and the production of pyruvate (Patterson et al., 2014; Wollheim and Maechler, 2002). Pyruvate enters the mitochondrion and act as substrate for pyruvate dehydrogenase and pyruvate carboxylase (Patterson et al., 2014; Wollheim and Maechler, 2002). This leads to the generation of reducing equivalents nicotinamide adenine dinucleotide (NADH) and flavin adenine dinucleotide ($FADH_2$) from the tricarboxylic acid (TCA), which then activates ETC (Wollheim and Maechler, 2002). Electrochemical proton gradient is then generated as the electrons are channelled through the complexes, and subsequently production of ATP from phosphorylation of ADP via ATP synthase as protons is channelled through (Patterson et al., 2014; Wollheim and Maechler, 2002). ATP-sensitive potassium channel (K^+_{ATP} channels) consist of the pore-forming subunit K^+IR 6.2 and the controlling sulfonylurea receptor 1 (SUR1) (Henquin, 2004). The binding of ATP to K^+IR 6.2 closes the channel, while binding of Mg ADP to SURI opens the channel (Henquin, 2004). Therefore, the increase in ATP/ADP ratio from glucose metabolism, endorses the closure of K_{ATP} channels and depolarization of the cytosolic membrane

(Henquin, 2004; Neye et al., 2006). This results in influx of Ca^{2+} inside the cell through the opened voltage-sensitive pump (Henquin, 2004; Neye et al., 2006; Wollheim and Maechler, 2002). Elevated Ca^{2+} concentrations trigger the insulin release via exocytosis (Henquin, 2004; Wollheim and Maechler, 2002) (Figure 2).

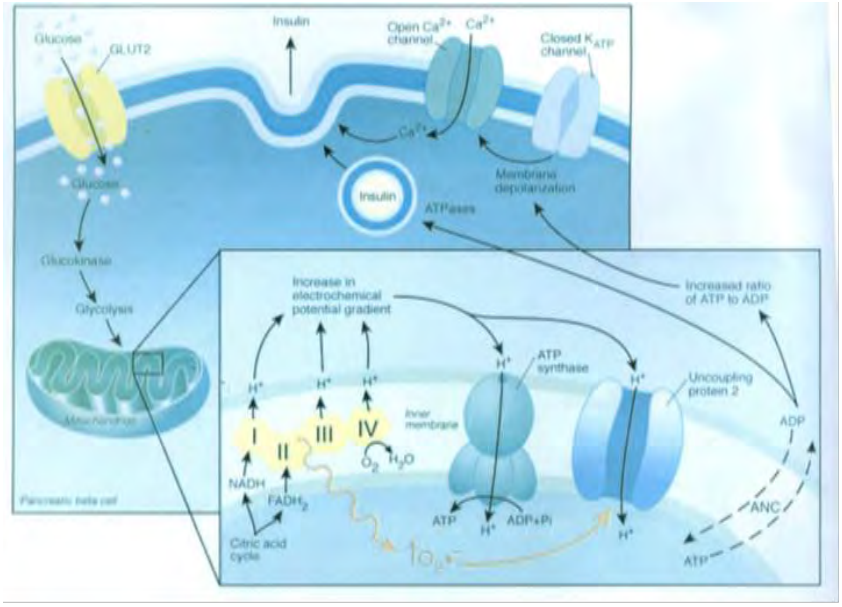

Figure 2: Overview of glucose metabolism for insulin secretion in the β-cells (Lowell and Shulman, 2005). Copyright permission for reproduction was granted from the author.

Reactive oxygen species induced by PIs have been suggested to impair insulin secretion by pancreatic β-cells (Chandra et al., 2009). It has been suggested that superoxide anions activate uncoupling protein 2 (UCP2) (Sakai et al., 2003); the inner membrane protein that dissipate the proton gradient before it can be used to provide ATP for oxidative phosphorylation (Kim et al., 2008; Krauss et al., 2003). The up-regulation of UCP2 causes partial depolarization of the mitochondrial membrane potential, decrease ATP production, block K_{ATP} channels and therefore, diminish insulin secretion.

In addition, hyperglycemia is also identified to increase oxidative stress and cause β-cell dysfunction (Sakai et al., 2003). Hyperglycemia has been reported to increase generation of ROS by affecting mitochondrial respiration chain in the pancreatic β-cells (Ahmadi et al., 2013; Sakai et al., 2003). It has been suggested that hyperglycemia increases generation of electron donors from Kreb Cycle NADH and $FADH_2$ (Lowell and Shulman, 2005; Maechler and Wollheim, 2001). This increases membrane potential as protons are pumped across the mitochondrial inner membrane (Lowell and Shulman, 2005; Maechler and Wollheim, 2001).

The inner membrane is proportional to electron flux through the respiration chain (Lowell and Shulman, 2005; Maechler and Wollheim, 2001). The electron transport at complex lll is then suppressed, hence increasing the half-life of free radical intermediates of coenzyme Q which then reduces oxygen to superoxide (Lowell and Shulman, 2005; Maechler and Wollheim, 2001). Increased mitochondrial superoxide activates UCP2-associated proton leakage leading to decreased ATP generation and insulin secretion (Brown et al., 2002; Echtay et al., 2002; Lowell and Shulman, 2005; Maechler and Wollheim, 2001). Zang et al., (2001) reported that UCP2 negatively controls insulin secretion and is a primary link between obesity, β-cell dysfunction and type 2 diabetes.

Dysfunctional or reduced pancreatic β-cell mass are the influential factors in the pathogenesis of type 2 diabetes and insulin resistance (Prentki et al., 2002; Unger, 1995). Overproduction of mitochondrial ROS endorses susceptibility to cell membranes damage and changing the mitochondrial permeability transition (Kim et al., 2008; Park and Han, 2014; Robertson et al., 2007). This could account for higher percentage of mitochondrial membranes depolarised and the release of apoptotic makers such as Bcl-2 family (proteins that controls mitochondrial permeabilisation through apoptosis) and cytochrome c (Park and Han, 2014; Robertson et al., 2007). This results in the formation of apoptosome with cytochrome c, apoptotic activating factor (Apaf)-1 and procaspase-9 (Shiozaki et al., 2002). The oligomerisation of procaspase-9 in apoptosome formed results in the activation of caspase-9 which in turn activates caspase-3 (Shiozaki et al., 2002). Activated caspase-3 leads to cell death characterized by chromatin condensation, nuclear fragmentation, DNA ladder and formation of apoptotic bodies (Shiozaki et al., 2002). It has been suggested that PIs should be co-administrared with the drugs used to reduce oxidative stress in order to reduce the risk of β-cell dysfunction and impairment of insulin secretion (Kalra et al., 2011; Rudich et al., 2001).

Currently, several clinical trials using antioxidant supplements such vitamin E and C have failed to establish significant improvement in oxidative stress markers in type 2 diabetic individuals (Matough et al., 2012; Savini et al., 2013). On the other hand, there is no laboratory or clinical data used sulfonylurea agents to evaluate if they can preserve pancreatic β-cell and improve insulin secretion in PI-treated patients. Glibenclamide is a well- known sulfonylurea receptor blocker, used to increase insulin secretion in pancreatic β-cells (Luzi and Pozza, 1997; Patane et al., 2000). It inhibits sulfonylurea receptor 1, the regulatory subunit of the K_{ATP} channels in pancreatic β-cells (Luzi and Pozza, 1997; Patane et al., 2000). This inhibition causes a cell membrane to depolarize and opens voltage-dependent Ca^{2+} channel (Luzi and Pozza, 1997; Patane et al., 2000). These outcomes in raise in intracellular Ca^{2+} in the β-cell and resultant stimulation of insulin release (Luzi and Pozza, 1997; Patane et al., 2000). Hence, the study hypothesized that insulin secretagogues could relieve oxidative stress by boosting insulin secretion and cellular anti-oxidant capacity.

However, plant derived antioxidants are becoming more promising as they can be used as nutritional supplements and have less side-effects (Savini et al., 2013). Naringin (4′, 5, 7-trihydroxy flavonone 7-rhamnoglucoside; Figure 3), flavanone glycoside of naringenin found in *Citrus paradisi* has been shown to possess potent antioxidant properties (Gopinath and Sudhandiran, 2012; Thangavel et al., 2012). Naringin has been demonstrated to have no known side-effects, as individuals have been consuming grapes and other citrus fruits for a long time (Thangavel et al., 2012). Naringin occurs naturally in citrus fruit and gives bitter flavour to some citrus fruits (Rajadurai and Stanely Mainzen Prince, 2006). It is rapidly hydrolysed to its glycoside naringenin by gut bacterial enzymes such as α-rhamnosidase and β-glucosidase (Amudha and Pari, 2011; Rajadurai and Stanely Mainzen Prince, 2006)

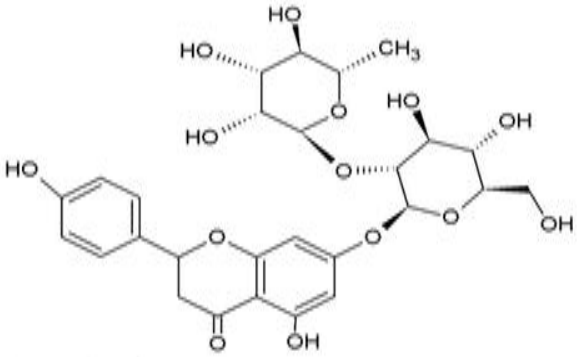

Figure 3: The structure of Naringin (4′, 5, 7-trihydroxy flavonone 7-rhamnoglucoside) (Sahu et al., 2014)**.** Copyright permission for reproduction was granted from the author**.**

Flavonoids have three chemical structures that confer on them their remarkable antioxidant properties; the hydroxyl groups attached to the aromatic ring structures of flavonoids, which allows them to undergo a redox reaction that helps to scavenge free radicals more easily; Certain structural groups which are capable of forming transition metal-chelating complexes that can regulate the production of ROS such as hydroxyl and oxygen radicals; Aromatic, heterocyclic rings and multiple unsaturated bonds, which enables delocalization system (Cavia-Saiz et al., 2010; Thangavel et al., 2012). Furthermore, naringin possesses metal-chelating complexes, antioxidant and free radical scavenging properties that have been reported to protect against lipid peroxidation (Gopinath and Sudhandiran, 2012).

Naringin has been demonstrated to ameliorate oxidative stress both *in vitro* and *vivo* studies. Amudha and Pari (2011) evaluated the valuable role of naringin on nickel induced nephrotoxicity and the findings showed that naringin treatment reversed the alterations in renal and urine markers, reducing lipid peroxidation and enhanced antioxidative cascade. All the alterations were supported by histopathological observations. Akondi et al (2011) showed a significant reduction of free radical generation in the testes of male rats that had undergone torsion when exposed to naringin. In addition, Thangavel et al., (2012) demonstrated that

naringin prevents liver damage, lipid peroxidation and preserves the antioxidant defence system in diethyl nitrosamine (DEN)-induced liver carcinogenesis in male Wistar rats. Furthermore, naringin has also been reported to possess pharmacological properties such as anti-inflammatory, anticancer, antimicrobial cholesterol lowering activities (Gopinath and Sudhandiran, 2012; Rajadurai and Stanely Mainzen Prince, 2006; Thangavel et al., 2012). Recent studies have reported that naringin also possessed antiapoptotic activities against ROS-induced injuries (Cavia-Saiz et al., 2010; Chen et al., 2014). Naringin has been shown to block mitogen-activated proteins kinases (MAPKs) pathway induced by oxidative stress in different cell lines (Kim et al., 2009). In human neuroblastoma, SH-SY5Y cells (Kim et al., 2009) and H9c2 cardic cells (Chen et al., 2014), naringin has been shown to inhibit JNK pathway against rotenone-induced apoptosis and hyperglycaemia-induced cytotoxicity respectively.

MAPKs are known as serine-threonine protein kinases essential for signal transduction from extracellular surface to the nucleus (Goillot et al., 1997; Wada and Penninger, 2004). They consist of extracellular signal-related kinases (ERKs), p38 MAPKs, c-Jun NH_2 terminal kinase (JNK) and stress-activated MAPKs (Goillot et al., 1997; Wada and Penninger, 2004). They are components of a three-kinase signalling regulate composed of the MAPK, MAPK kinase (MAP2K) and MAPK kinase (MAPK3K) (Goillot et al., 1997; Wada and Penninger, 2004). These MAPK pathways regulate diverse cellular functions such as cell differentiation, proliferation, migration and apoptosis (Wada and Penninger, 2004). Studies have demonstrated that oxidative stress trigger MAPK pathway but the mechanism is not fully understood (Chen et al., 2014). However, it has been suggested that overproduction of ROS tends to oxidize intracellular kinases (e.g. MAP3Ks) that are involved in MAPK signalling cascade (Chen et al., 2014). Apoptosis signal-regulating kinase 1 (ASK-1) is an associate of the MAP3K super-intimate for JNK and p38. It oxidises the reduced thioredoxin and oxidize thioredoxin disassociate from ASK-1 leading to the stimulation of JNK and p38 pathway via

oligomerization of ASK-1 (Chen et al., 2014). Stimulated JNK causes the release of apoptogenic factors such as cytochrome c and second mitochondrial-derived activator of caspases (smac)/DIABLO from the mitochondrial therefore initiating apoptosis, whereas p38 is involved in the phosphorylation of Bcl2 family and stimulation of the mitochondrial apoptotic pathway (Chen et al., 2014). Based on these findings, it is therefore postulated that naringin could ameliorate the impairment of insulin secretion and preserve pancreatic β-cell integrity by reducing oxidative stress.

1.6 Aim and Objectives

To investigate whether naringin could reverse HIV-1 protease inhibitors-associated pancreatic β-cell dysfunction with respect to: glucose-induced insulin secretion, β-cell viability, oxidative stress and β-cell antioxidant defence systems in rat insulinoma cell lines (RIN-5F) *in vitro*.

CHAPTER TWO

2. Materials and Methods

2.1 Chemicals and reagents

The rat insulinoma cell lines (RIN-5F) were purchased from European Collection of Cell Cultures (ECACC). All cell culture reagents, the PIs (nelfinavir, saquinavir, atazanavir, glibenclamide) naringin, glucose and the Super Oxide Dismutase (SOD) assay kit were purchased from Sigma Chemical (St Louis, MO). ATP assay kit was purchased from Biovison (Mountain View, CA). The GSH-Glo^{TM} Glutathione assay was obtained from Whitehead Scientific (Johannesburg, South Africa). Caspase-Glo$^{®}$-9 assay kit was purchased from Promega (Madison, USA) and caspase-3 fluorescence kit was bought from Cayman Chemical Company (Canada, USA). Rat insulin ELISA kit was purchased from Alpha Diagnostics (Salem, NH).

2.2 Cell culture

The RIN-5F cells were cultured within 40 passages in 75 cm^3 flasks in RPMI-1640 medium containing 11.1 mM glucose supplemented with 10% Fetal Bovine Serum (FBS), 10% penicillin-streptomycin, 10.0 mM HEPES and 1.0 mM sodium pyruvate. The cultures were maintained at 37°C in humidified with 5% CO_2.

2.3 Trypsinisation and cell counting

Trypsinisation process was done to detach cells from the culturing vessel once they reached 80% confluency, and also to sub-culture and seed the cells for the various biochemical assays. This process involved rinsing the cells three times with warm 0.1M PBS (3 ml; 37°C) and incubating the cells with trypsin-EDTA (1 ml) for 2 min. The cells were then observed for roundness using an inverted light microscope (Olympus IXSI; 20 x). Once they were found to

be round, trypsin was discarded and CCM (5 ml) added to the flask. The flask was agitated to removed cells from culturing vessel and the cell suspension was counted using haemocytometer. Trypan blue (0.4%) was applied in a dye exclusion procedure for cell counting. The principle of dye exclusion is based on damaged/dead cell membranes which allow entry of the dye into the cells and the cells stain blue whereas sustainable cells remain unstained.

2.4 Protease Inhibitors (PIs) preparation

Nelfinavir (Viracept) and saquinavir (Inviraset) were initially dissolved in ethanol (100%, w/v) to a stock concentration of 10.0 mg/ml (15 mM) and 2.0 mg/ml (2.6 mM) respectively. Atazanavir (Reyatazt) was dissolved in de-ionized water to a stock concentration of 4 mg/ml (7.3 mM). Glibenclamide was dissolved in dimethylsulfoxide (DMSO) to a final concentration of 20.0 mM, and naringin was dissolved in DMSO to a stock concentration of 20 mg/ml (5 mM).

2.5 Cell exposure

To measure the effects of PIs on insulin levels, the cells were plated in 6-wells plates (5.0×10^5 cells/well) in the presence of 11 mM glucose only and allowed to grow to 80% confluence, followed by treatment with nelfinavir (0.0, 1.0, 2.5, 5.0, 7.5 and 10 μM), saqanavir (0.0, 1.0, 2.5, 5.0, 7.5 and 10 μM), atazanavir (0.0, 5.0, 10.0, 15.0, 20.0 and 25.0 μM) for 24 hr. To measure glucose-induced insulin secretion, cells were similarly exposed to nelfinavir (10.0 μM), saquinavir (10.0 μM), atazanavir (20.0 μM), nelfinavir (10.0 μM) plus glibenclamide (10.0 μM), saquinavir (10.0 μM) plus glibenclamide (10.0 μM) and atazanavir (20 μM) plus glibenclamide (10 μM) at 11, 15, 20 and 25 mM glucose, respectively for 24 hr. Vehicle controls constituted Cell Culture Medium (CCM) with or without glibenclamide (10.0 μM) were applicable.

To measure the dose-dependent of naringin on insulin secretion, cells were similarly plated in 6-wells plates (5.0×10^5 cells/well) in the presence of 11 mM glucose only, allowed to grow to 80% confluence, followed by treatment with naringin (0.0, 10.0, 20.0, 30.0, 40.0 and 50 μM) for 24 hr.

To investigate the role of PIs relative to naringin on RIN-5F cells, cells were exposed to nelfinavir (10.0 μM), saquinavir (10.0 μM), atazanavir (20.0 μM), nelfinavir (10.0 μM) plus naringin (10.0 μM), saquinavir (10.0 μM) plus naringin (10.0 μM) and atazanavir (20 μM) plus naringin (10 μM) in the presence of 11 mM glucose only for 24 hr. Vehicle controls constituted CCM with or without naringin (10.0 μM) were applicable.

For lipid peroxidation, ATP and caspase-3 and -9 assays, cells were cultured to 90% confluency in $25cm^2$ tissue flasks and treated with test compounds. For the GSH assay, the cells (1.0×10^4 cells/well) were plated in 96-well microtiter plates and allowed to attach overnight, and similarly treated with test compounds. After the treatments, cells were harvested and subjected to biochemical assays for profile analysis.

2.6 Biochemical Analysis

2.6.1 Insulin ELISA

Rat Ultrasensitive ELISA was used to measure insulin secretion as per manufacturer's instructions. In brief, the cells were incubated with Krebs Ringer Bicarbonate Buffer (KRBB- 140 mM NaCl, 3.6 mM KCl, 0.5 mM NaH_2PO_4, 0.5 mM $MgSO_4$, 1.5 mM $CaCl_2$, 10 mM HEPES, 2 mM NaHCO3, pH 7.4) with 0.1% BSA in duplicates for 5 min, followed by stimulation with 0-25 Mm glucose in KRBB with for 0.1% BSA for 30 min at 37ºC. The supernatant was collected, centrifuged at 12000 x g for 10 mins at 4ºC and the cells lysed to determine the protein content by Bradford method as previously described (Bradford, 1976). Twenty five µl of standards, supernatant from controls and samples were added to the primary antibody coated wells of the ELISA. Enzyme conjugated 1 x solution (100 µl) was added into each well and incubated the plate on a shaker at 800 rpm for 2.0 hr at room temperature (18-25 °C). After 6 times washes with buffer, 200 µl of substrate TMB was added into each well and incubated in a dark for 15 min at room temperature. The reaction was then stopped by adding 50 µl of stop solution to each well, mixed well on a shaker (700 rpm) for 5 sec. And the absorbance was read at 450 nm using EZ read 400 microplate reader (Biochrom Ltd, Cambridge, UK). The values obtained from standard curve were expressed as ng of insulin secretion per mg of total cellular protein.

2.6.2 ATP assay

The ATP quantification assay used in this study used bioluminescence as per the manufacturer's instructions. This assay is constructed on the conversion of a luciferase-inactive derivative to D-luciferin in the presence of $Mg^{2+.}$ Luciferase substrate reacts with luciferase to produce oxyluciferin and yield ATP in form of luminescence (Figure 4). This luminous signal is directly proportional to the concentration of ATP existing in the cells.

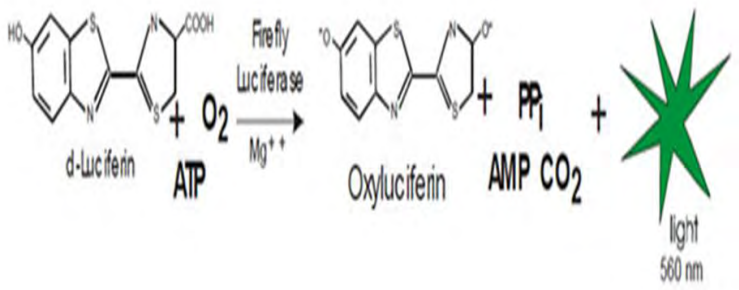

Figure 4: Principle of the ATP assay for the quantification of cellular ATP (Schafer et al., 2009). Copyright permission for reproduction was granted from the author.

ATP levels were measured using EnzyLight ^{TM} ADP/ATP Ratio Assay kit. Cells (10^4/well) were cultured in white opaque microplate in triplicates, trypsinized and respendend in 10 µl of culture medium. ATP reagent (90 µl) which was prepared acccording to manufactures guidelines was then added into each well and mixed by tapping the plate. After incubation for 1 min at room temperaturel light signal relative to the cellular ATP content was detected on Modulus^{TM} microplate luminometer (Turner Biosystems, Sunnyvale, USA). The values obtained were expressed as mean relative light units (RLU).

2.6.3 Oxidative stress assay

Malondialdehyde (MDA) is the end product of lipid peroxidation and an indicator of oxidative stress. This technique is based on the reaction of two molecules of Thiobarbturic Acid (TBA) with one molecule of MDA to form pink colour (Figure 5), then the MDA concentration can be measured by microliter plate reader.

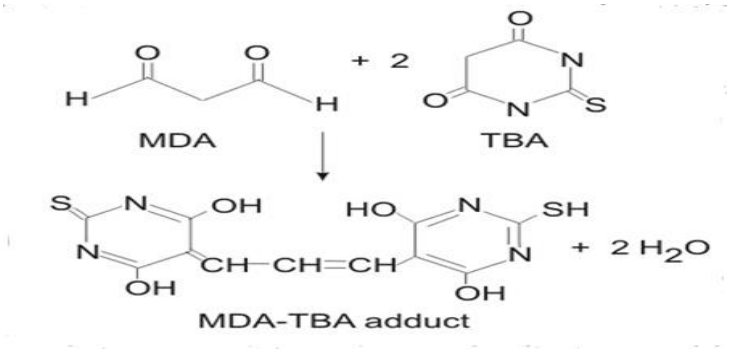

Figure 5: The reaction of malondialdehyde with thiobarbituric acid (Cayman Chemical Protocol).https://www.google.co.za/search?q=The+reaction+of+malondialdehyde+with+thiobarbituric+acid&biw=939&bih=403&source=lnms&tbm3B385

To investigate the PIs-mediated generation of reactive oxygen species (ROS), Thiobarbituric acid reactive substances (TBARS) assay was used to assess the levels of MDA according to the modified method of Halliwell and Chirico (1993). After 24 hr treatment, 100 µl of supernatant from each treated well and controls were aliqouted into glass tubes in triplicates.

In another set of test tubes, 200 µl of serially diluted MDA standard was added to 500 µl of 2% H_3PO_4, 400 µl of 7% H_3PO_4 and 400 µl of BHT/TBA solutions, respectively. Reactions in both sets of tubes were initiated with 200 µl of 1M HCl. All the tubes were incubated in a shaking boiling water bath (100 °C) for 15 min and allowed cooled at room temperature. n-Butanol (1.5 ml) was then added to each tube and thoroughly mixed then centrifuged (13000 rpm, 24 °C, and 6 min) before 100 µl of the top phase was transferred to a 96-well micro-plate in triplicates and read at 532 nm and 600 nm using Spectrostar ® micro-plate reader (Biochrom Ltd, Cambridge, UK). The plasma MDA concentrations were calculated using an extinction coefficient of 1.56×10^5 M^{-1} cm^{-1}.

2.6.4 Superoxide dismutase assay

SOD enzymes catalyses the dismutation of superoxide anion into hydrogen peroxide and oxygen molecule, thus reduces the cytotoxic. SOD assay measures SOD activity *in vitro*. This technique uses WST-1 that produces a water-soluble formazan product as superoxide anions are being reduced. The rate of reduction with a superoxide anion is directly proportional to the xanthine oxidase activity, and is reserved by SOD activity (Figure 6).

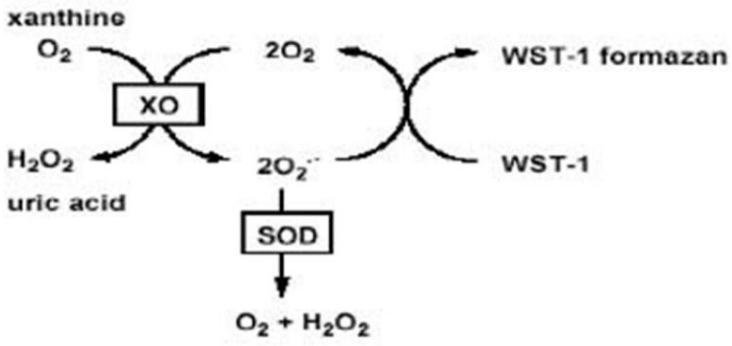

Figure 6: The principle of determination of SOD activity by SOD assay (Sigma Chemical Protocol).https://www.google.co.za/?gfe_rd=cr&ei=2Tv0VKXYL5Cp8wfkk4GoBw&gws_rd=ssl#q=The+principle+of+determination+of+SOD+activity+by+SOD+assay+

Superoxide dismutase activity was assessed using SOD assay. Following treatment, RIN-5F cells (1.0×10^4) were washed with cold 0.1 M Phosphate Buffer Saline (PBS) then added 0.5 ml of cold lysis buffer (2.5M NaCl, 100 mM EDTA, 1% Triton X-100, 10 mM Tris (pH 10) and 10% DMSO). After 10 min on ice, the lysate was centrifuged at 12, 000 × g for 5 min at 4º C). Supernatant (20 µl) was then added in triplicates to the wells in a 96-well microtitre plate. Water-Solution tretrazolium and enzyme working solutions were prepared according to manufacturer's guidelines. Water-Solution tretrazolium solution (200 µl) was then added each well followed by 20 µl of enzyme working solution incubated at 37°C for 20 min. Absorbance was measured at 450 nm using EZ 400 reader microplate (Biochrom Ltd, Cambridge, UK).

Sample concentrations were extrapolated from standard curve and values were expressed in units of enzyme normalized to cellular protein in milligram (mg).

2.6.5 GSH-Glo™ Glutathione Assay

Glutathione (GSH) is a tripeptide (cysteine, glycine and glutamine) that plays a role in the detoxification of electrophilic and peroxide species. This assay is based on the conversion of luciferin derivative (Luc-NT) into luciferin in the presence of glutathione, catalysed by GST. The light signal that is produced is coupled to luciferase reaction, proportional to the quantity of glutathione that is present (Figure 7).

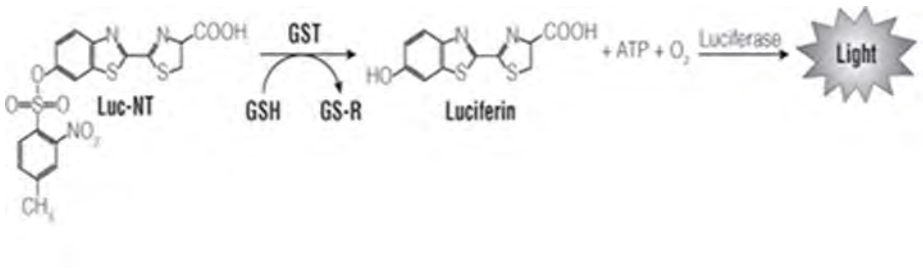

Figure 7: The principle of the GSH-Glo™ Glutatione assay (Promega Protocol). http://www.promega.com/~/media/Files/Resources/Protocols/Technical%20Bulletins/101/GSH-Glo%20Glutathione%20Assay%20Protocol.pdf

Glutathione-Glo™ Assay (Promega) was used according to manufacturer's recommendations to quantify intracellular glutathione levels. Harvested cells suspensions were diluted in 0.1 M PBS and 50 µl (10^5 cells/well) dispensed into 96 well plate in triplicates followed by 50 µl of GSH-Glo™. The reagents were mixed well by shaking on a mechanical shaker then incubated at room temperature for 30 min. To each well was then added 100 µl of reconstituted Luciferin Detection Reagent, mixed briefly on a plate shaker then incubated for 15 min at room temperature. Glutathione standards (0-5 µM) were prepared from a 5 mM stock diluted in

deionized water. Luminescence was detected on a Modulus™ microplate luminometer (Turner Biosystems, Sunnyvale, USA). GSH concentrations in each sample were extrapolated from the standard curve and expressed as mean Relative Light units (RLU).

2.6.6 Analysis of apoptotic markers

2.6.6.1 Caspase-Glo®-9 assay kit

Caspase-Glo® 9 assay is a luminescent assay that measures activity of caspase-9. This assay is based on the cleavage of substrate Ac-LEHD-p-NA by active caspase-9. Then, the luminescent signal generated through mono-oxygenation of amino-luciferin can be quantified on a Modulus™ microplate luminometer (Figure 8). The luminescent signal generated is directly proportional to the level of caspase activity present inside the cell.

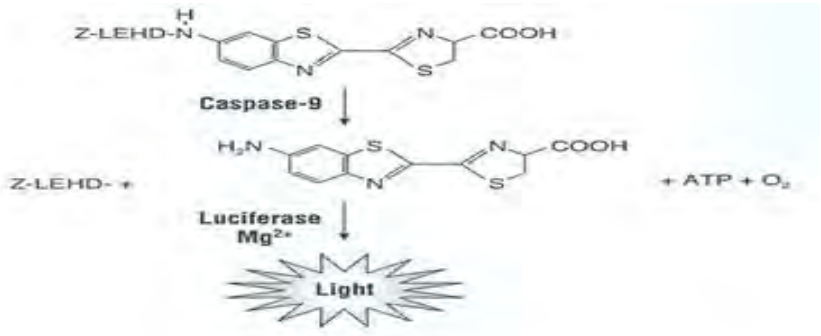

Figure 8: The principle for the detection of caspase-9 activity (Promega Protocol). https://worldwide.promega.com/~/media/files/resources/protocols/technical%20bulletins/101/caspase-glo%209%20assay%20protocol.pdf

RIN-5F cells (1.0×10^4) were seeded into an opaque polystyrene 96-well microtitre plate in triplicates. Following treatment, Caspase-Glo® 9 reagent was prepared according to manufacturer's instructions then added 100 µl of Caspase-Glo® 9 reagent to each well. The plate placed on a shaker (300-500 rpm) for 30 seconds and incubated in the dark for 30 min at

room temperature. Luminescence was measured on a Modulus™ microplate luminometer. The data was expressed as relative light units (RLU).

2.6.6.3 Caspase-3 fluorescence assay kit

Caspase-3 fluorescence assay measures the activity of caspase-3. This assay is based on the cleavage of specific caspase-3 substrate, N-Ac-DEVD-MC-R110 by active caspase-3, which then generates a fluorescent product that can be quantified using excitation and emission wavelength of 485 and 535 nm (Figure 10). The fluorescent signal produced is directly proportional to the level of caspase activity present inside the cell.

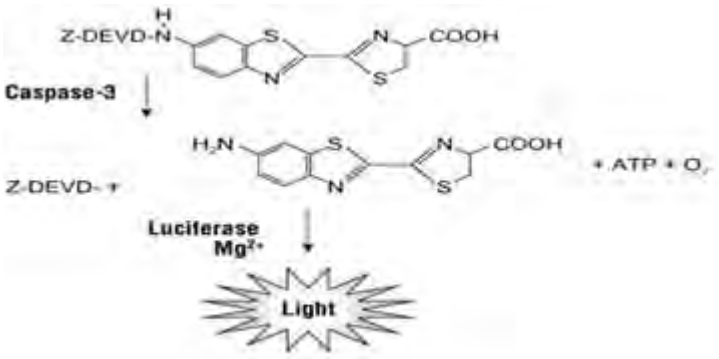

Figure 9: Principle for the detection of caspase-3 activity (Cayman Chemical Protocol). https://worldwide.promega.com/~/media/files/resources/protocols/technical%20bulletins/101/caspase-glo%203%207%20assay%20protocol.pdf

RIN-5F cells (5×10^4) were seeded in a 96-well plate for the assay of caspase-3 activities using caspase-3 fluorescence assay according to manufacturer's recommendations. Caspase-3 assay buffer (200 µl) was then added to each well in triplicates and centrifuge (800 × g, 5 min) at room temperature. The supernatant from each well was aspirated and cell-based assay buffer (100 µl) added and the plate incubated with gentle shacking on an orbital shaker for 30 min at

room temperature. The plate was then centrifuged at 800 × g for 10 min at room temperature and 90 µl of the supernatant was transferred from each well to a corresponding 96-well plate. Caspase -3 inhibitor solution (10 µl) was then added to appropriate wells, followed by addition of active capsase-3 standards (100 µl) into the corresponding wells. Thereafter, 100 µl of caspase-3 substrate solution was added to each well and the plate incubated at 37°C for 30 min. The fluorescence intensity was then measured on a Modulus™ microplate luminometer at the excitation of 485 nm and emission of 535 nm.

3.0 Statistical analysis

The data are presented as mean ± SD and analysed by Graph pad Prism Software Version 5.0. Mann-Whitney tests and/or Student t-tests were applied to the results to determine statistical significance. $P \leq 0.05$ was considered as statistically significant.

CHAPTER THREE

Results

3.1 Insulin ELISA

Increasing concentrations of glucose (11-25 mM) caused increased levels of insulin secretion in cells with or without PIs and/or glibenclamide (Figure 10 A and B). However, insulin secretions at all glucose concentrations were significantly ($p < 0.05$) lower in the presence of different PIs (nelfinavir, saquinavir and atazanavir) compared to the control group. However, there was no significant difference in insulin secretion among the different PIs individually (Figure 10 A).

Similarly, insulin secretion by RIN-5F cells at all glucose concentrations were significantly ($p < 0.05$) lower in the presence of both PIs and glibenclamide compared to treatment with glibenclamide alone. There was no significant difference in insulin secretion among combination of single PIs with glibenclamide (Figure 10 B).

Furthermore, insulin secretion by cells at different glucose concentrations was higher in the presence of glibenclamide and also in combination with different PIs plus glibenclamide (Figure 10 A and B) compared to PI-treated cells only.

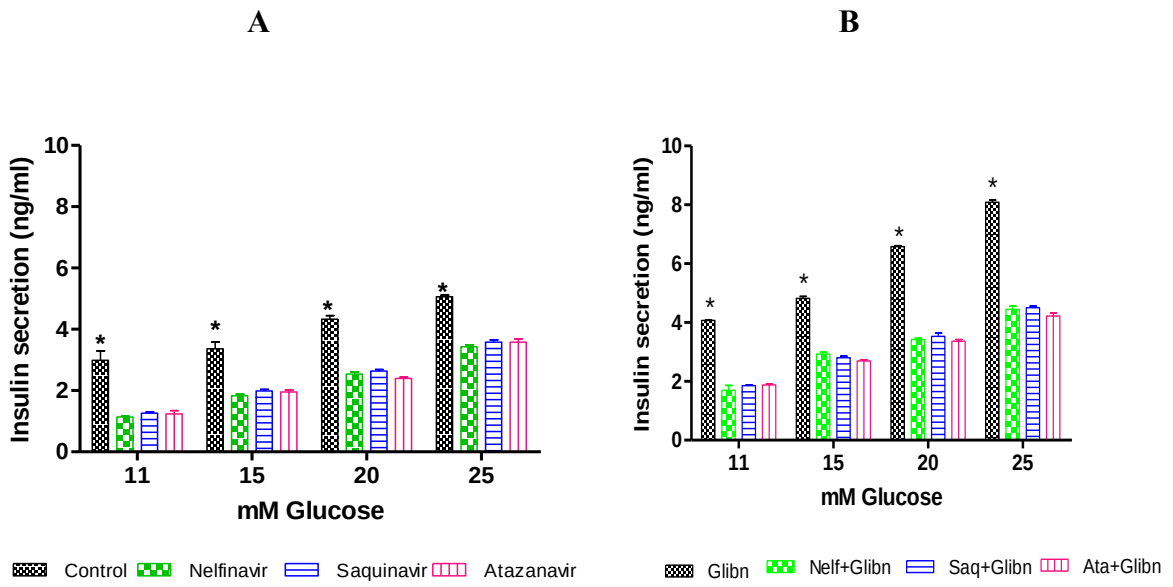

Figure 10: Glucose-induced insulin secretion in cells that were treated with (A) PIs and/or (B) glibenclamide. (*$p < 0.05$ compared to controls, respectively).

3.2 ATP assay

Increasing concentrations of glucose from 11 to 25 mM caused increases in the levels of ATP in cells with or without PIs or glibenclamide (Figure 11 A and B). However, ATP levels at all glucose concentrations were significantly ($p < 0.05$) reduced in the presence of PIs (nelfinavir, saquinavir and atazanavir) compared to the control groups (without PIs) (Figure 11 A).

Similarly, ATP levels at all glucose concentrations were significantly reduced in the presence of PIs plus glibenclamide compared to treatment with glibenclamide alone (Figure 11 B). Saquinavir was associated with significantly ($p < 0.05$) less ATP production with or without glibenclamide compared to nelfinavir or atazanavir (Figure A and B).

Finally, ATP levels in cells at different glucose concentrations were higher in the presence of glibenclamide than without glibenclamide and with different PIs plus glibenclamide (Figure 12 A and B).

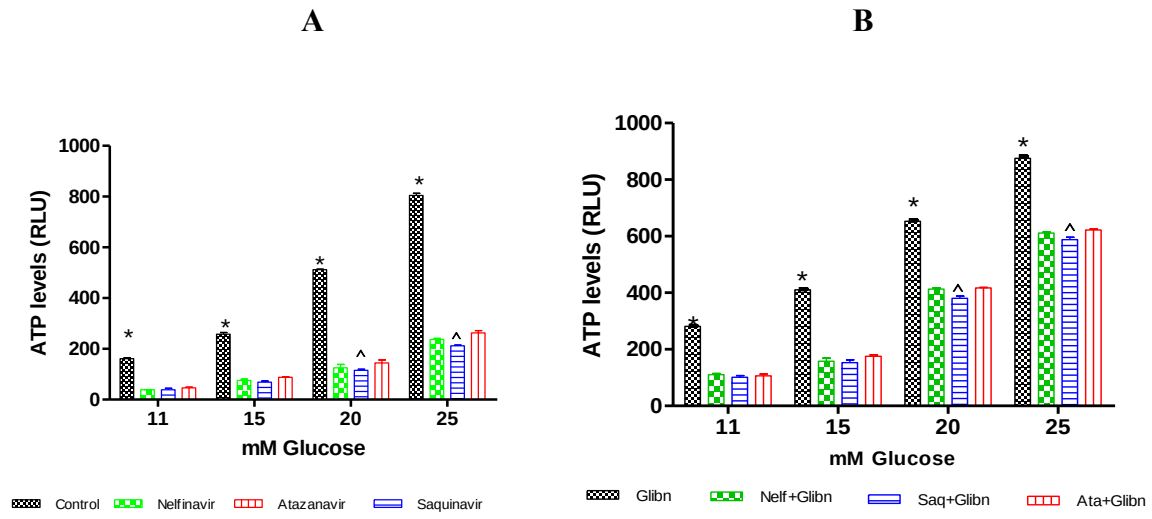

Figure 11: ATP productions after cells were treated with (A) PIs and/or (B) glibenclamide at different concentrations of glucose. (*$p < 0.05$ when compared to controls, ^$p < 0.05$ compared to nelfinavir and atazanavir, respectively).

3.3 Insulin ELISA

The insulin secretion was measured in RIN-5F cells exposed to different concentrations of PIs; (nelfinavir (1-10 µM), saquinavir (0-10 µM) and atazanavir (5-20 µM) for 24 h. Linear regression analysis showed significant decrease in insulin levels in response to nelfinavir, saqunavir and atazanavir (r^2= 0.86, 0.76, 0.95, respectively) in a dose-dependent manner (Figure 12). However, atazanavir appears to have a more enhanced suppressive effect on insulin secretion compared to nelfinavir and saquinavir.

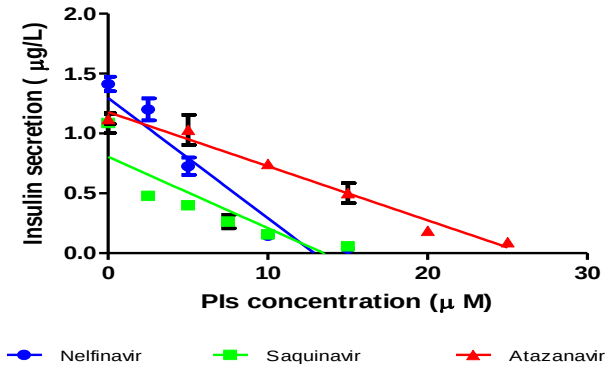

Figure 12: Linear regression analysis of concentration-depend inhibition of insulin secretion in RIN-5F cultured cells. Nelfinavir: r^2 = 0.86; saquinavir: r^2 0.76 and atazanavir: r^2 = 0.95

3.4 Lipid peroxidation

There was a significant increase in MDA levels as glucose concentration increased from 11 mM to 25 mM with or without PI or with PI plus glibeclamide but not in the presence of glibenclamide alone. The MDA levels at all glucose concentrations were significantly ($p < 0.05$) higher in the presence of different PIs compared to the controls (Figure 13 A). The MDA levels in the presence of the different PIs was not statistically significantly different at all glucose concentrations, except at 25 mM where atazanavir caused a significantly ($p < 0.05$) lower MDA concentrations compared to nelfinavir and saquinavir (Figure 13 A).

Furthermore, MDA levels at all glucose concentrations were significantly higher in the presence of the PIs plus glibenclamide compared to treatment with glibenclamide alone (Figure 13 B). At 25 mM glucose concentration, atazanavir plus glibencamide caused a significantly lower MDA concentrations compared to nelfinavir plus glibenclamide and saquinavir plus glibenclamide while MDA concentration of the different PIs plus glibenclamide did not differ statistically at other glucose concentrations (Figure 13 B). Glibenclamide blunted lipid peroxidation at all glucose concentration.

Finally, MDA levels at different glucose concentrations were lower in the presence of glibenclamide than without glibenclamide or with different PIs (Figure 13 A and B)

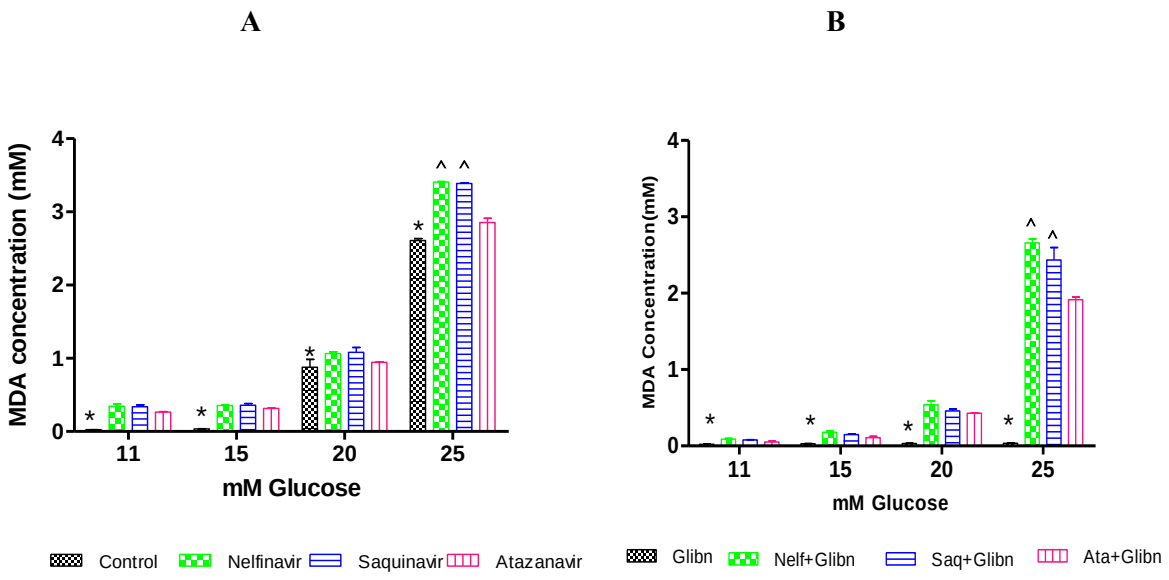

Figure 13: TBARS assay measured as MDA concentrations after cells were treated with (A) PIs and/or (B) glibenclamide at different concentrations of glucose. (*$p < 0.05$ when compared to controls, respectively, ^$p<0.05$ compared to nelfinavir and saquinavir).

3.5 Superoxide dismutase (SOD) assay

Total SOD activities significantly ($p < 0.05$) increased with increased glucose concentrations (11-25 mM) and also with exposure to nelfinavir, saquinavir and atazanavir compared to controls, respectively (Figure 14 A). However, after treatment with glibenclamide SOD activities significantly ($p < 0.05$) increased in controls but decreased in cells that were treated with nelfinavir, saquinavir or atazanavir (Figure 14 B).

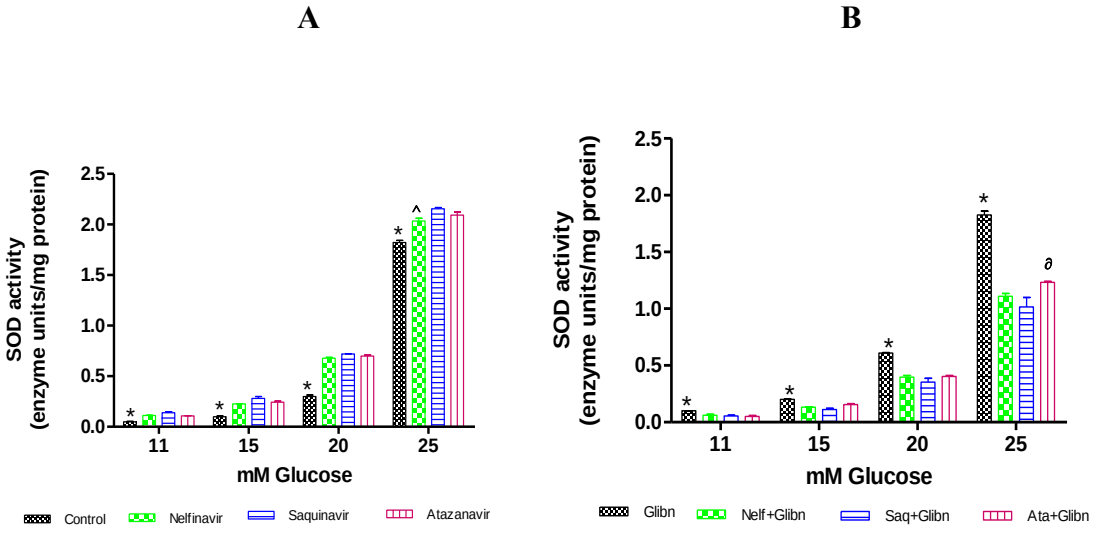

Figure 14: SOD activity after cells were exposed with (A) PIs and/or (B) glibenclamide at different concentrations of glucose. (*, ^, ∂ $p<0.05$ when compared to controls, nelfinavir and saquinavir or saquinavir, respectively).

3.6 Glutathione (GSH) assay

GSH concentrations were significantly reduced ($p < 0.05$) in cells that were exposed to PIs compared to controls as glucose concentration increased (Figure 15 A). However, at 11 mM glucose, controls had higher levels of GSH which dropped as glucose concentration increased. In PI-treated cells, GSH levels were low then increased to maximum at 15 mM glucose concentration then decreased glucose concentration increases. There was no difference observed in GSH levels between the control and PIs at 25 mM glucose (Figure 15 A).

Glibenclamide significantly ($p < 0.05$) increased GSH levels in a glucose dose-dependent manner (Figure 15 B). Co-treatments (nelf+glibn, saq+glibn and ata+glibn) had an increased GSH levels respectively in a dose-dependent manner compared to PIs only.

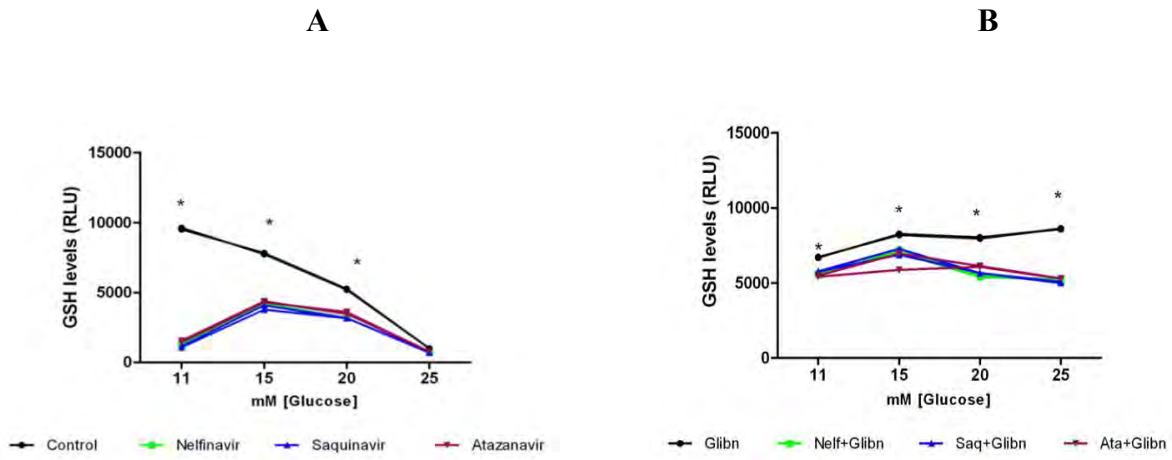

Figure 15: Glutathione levels after cells were exposed with (A) PIs and/or (B) glibenclamide at different concentrations of glucose. (*$p < 0.05$ when compared to controls, respectively).

3.7 Caspase assays

3.7.1 Caspase-3 Fluorescent assay

Caspase-3 activities increased with glucose concentrations in the medium. There was no significant ($p < 0.05$) difference in caspase-3 activities in control and glibenclamide-treated cells at baseline glucose concentrations (11 mM). However, at higher glucose concentrations (20-25 mM), glibenclamide significantly ($p < 0.05$) reduced caspase-3 compared to controls. Nelfinavir, saquinavir and atazanavir all exhibited increases in caspase-3 activities while in the presence of glibenclamide, the activities were significantly ($p < 0.05$) decreased in a glucose-dependent manner, respectively (Table 2)**.**

Table 2: Caspase-3 activities expressed as Relative Fluorescence Units (RFU) in RIN-5F cells treated with PIs and glibenclamide at different concentrations of glucose.

Mean ± SD					
Glucose Mm		11	15	20	25
Control		317.1 ± 4.2	330 ± 0.6	632.7 ± 31.6	748.2 ± 4.1
	Glibenclamide	313.4 ± 11.5	368.5 ± 29.0	327.6 ± 8.5*	340.8 ± 11.0*
Nelfinavir		613.2 ± 16.9$^{\#1}$	1354 ± 71.8$^{\#1}$	3115 ± 23.0$^{\#1}$	4113 ± 129.1$^{\#1}$
	Glibenclamide	451.1 ± 5.6$^{\#}$	857.7 ± 5.5$^{\#}$	932.6 ± 31.7$^{\#}$	1233 ± 31.3$^{\#}$
Saquinavir		688.1 ± 11.3$^{\wedge 1}$	1469 ± 32.4$^{\wedge 1}$	3399 ± 31.4$^{\wedge 1}$	4343 ± 59.0$^{\wedge 1}$
	Glibenclamide	429.5 ± 4.8$^{\wedge}$	929.9 ± 16.5$^{\wedge}$	1131 ± 127.2$^{\wedge}$	1317 ± 23.8$^{\wedge}$
Atazanavir		671.1 ± 8.4$^{\theta 1}$	1400 ± 1.5 $^{\theta 1}$	3042 ± 57.0 $^{\theta 1}$	4249 ± 49.74$^{\theta 1}$
	Glibenclamide	498.6 ± 13.4$^{\theta}$	749.5 ± 38.9$^{\theta}$	939.1 ± 63.7$^{\theta}$	1210 ± 4.2$^{\theta}$

*, $^{\#1}$, $^{\wedge 1}$, $^{\theta 1}$ $p < 0.05$ compared to the controls; $^{\#}$, $^{\wedge}$, $^{\theta}$ $p < 0.05$ compared to nelfinavir, saquinavir and atazanavir, respectively

3.7.2 Caspase-Glo® 9 assay

Caspase-9 activities increased with glucose concentrations increased from in the medium. There was no significant ($p < 0.05$) difference in caspase-9 activities in control and glibenclamide-treated cells at baseline glucose concentrations (11 mM). Nevertheless, at higher glucose concentrations (20-25 mM), glibenclamide significantly ($p < 0.05$) reduced caspase-9 activities compared to controls. All PIs (nelfinavir, saquinavir and atazanavir) exhibited increases in caspase-9 activities while in the presence of glibenclamide, the activities were significantly ($p < 0.05$) decreased in a glucose-dependent manner, respectively (Table 3).

Table 3: Caspase-9 activities Relative Light Units (RLU) x 10^2 in RIN-5F cells treated with PIs and glibenclamide at different concentrations of glucose.

Mean RLU ± SD					
Glucose Mm		11	15	20	25
Control		125.70 ± 35.91	145.80 ± 6.449	310.10 ± 1.322	472.90 ± 91.58
	Glibenclamide	100.80 ± 1385	122.40 ± 0.7*	270.10 ± 28.38*	353.90 ± 2.291
Nelfinavir		281.90 ± 45.64$^{\#1}$	380.20 ± 15.91$^{\#1}$	758.40 ± 65.27$^{\#1}$	1485 ± 41.73$^{\#1}$
	Glibenclamide	175.30 ± 21.46$^{\#}$	286.50 ± 7.283$^{\#}$	489.20 ± 91.97$^{\#}$	705.60 ± 19.76$^{\#}$
Saquinavir		320.70 ± 15.11$^{\wedge 1}$	458.80 ± 20.73$^{\wedge 1}$	834.3 ± 53.92$^{\wedge 1}$	1566 ± 13.76$^{\wedge 1}$
	Glibenclamide	216 ± 6.06$^{\wedge}$	299.20 ± 15.27$^{\wedge}$	445.50 ± 73.91$^{\wedge}$	742.10 ± 17.67$^{\wedge}$
Atazanavir		283.10 ± 15.63$^{\theta 1}$	425.60 ± 7.775 $^{\theta 1}$	715.60 ± 11.02$^{\theta 1}$	1353 ± 19.70$^{\theta 1}$
	Glibenclamide	165.20 ± 47.96$^{\theta}$	281.60 ± 24.77$^{\theta}$	475.80 ± 44.94$^{\theta}$	666.70 ± 16.16$^{\theta}$

*, $^{\#1}$, $^{\wedge 1}$, $^{\theta 1}$ $p < 0.05$ compared to the controls; $^{\#}$, $^{\wedge}$,$^{\theta}$ $p < 0.05$ compared to nelfinavir, saquinavir and atazanavir, respectively

3.8.0 Naringin

3.8.1 The effect of naringin on insulin secretion

Insulin secretion increased with naringin concentrations. Linear regression analysis showed significant correlation (r^2 = 0.9589, 95% Cl= 0.01490 to 0.02692) (Figure 16).

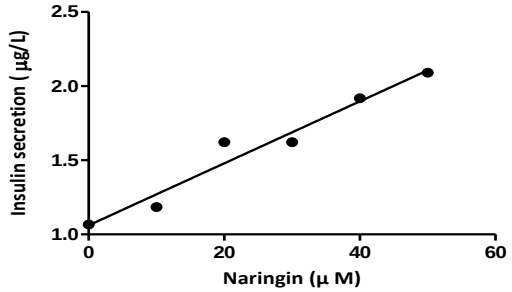

Figure 16: A dose-dependent increase insulin secretion in cells after naringin (0-50 µM) treatment for 24 h at 11 mM glucose concentration.

3.8.1 The effect of naringin on lipid peroxidation.

The MDA concentrations on PI exposure were higher ($p < 0.0001$) compared to untreated controls (Figure 17) at 11 mM glucose concentrations. However, the combination of naringin plus PI treatment significantly (narg+nelf; $p < 0.0001$, narg+saq; $p < 0.0001$ and narg+ata; $p < 0.0001$) reduced MDA concentrations compared to the respectively cells treated with PIs alone, respectively There was no significant difference in MDA concentrations between naringin and controls.

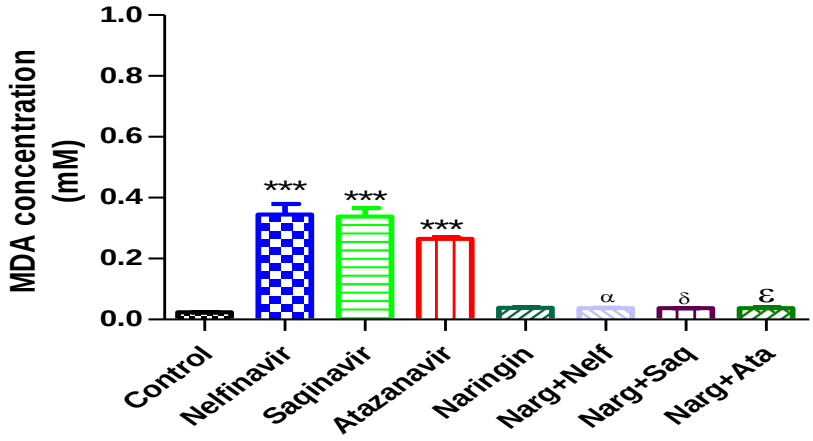

Figure 17: Malondialdehyde levels in RIN-5F cells treated with PIs and/ or naringin (10 µM) for 24 h at 11 mM glucose concentration. (***$p < 0.0001$ compared to controls, $^{\alpha}p < 0.0001$ compared to nelfinavir, $^{\delta}p < 0.0001$ compared to saquinavir and $^{\varepsilon}p < 0.0001$ compared to atazanavir respectively)

3.8.2 The effect of naringin on antioxidants (superoxide dismutase)

The SOD activity in PIs exposure was significantly ($p < 0.0001$) increased compared to controls (Figure 18). However, the combined treatment of naringin plus different PIs significantly (narg+nelf; $p < 0.0001$, narg+saq; $p < 0.0001$ and narg+ata; $p < 0.0001$) reduced SOD activities compared to the cells treated with PIs alone. There was no significant difference in SOD activities between naringin and control.

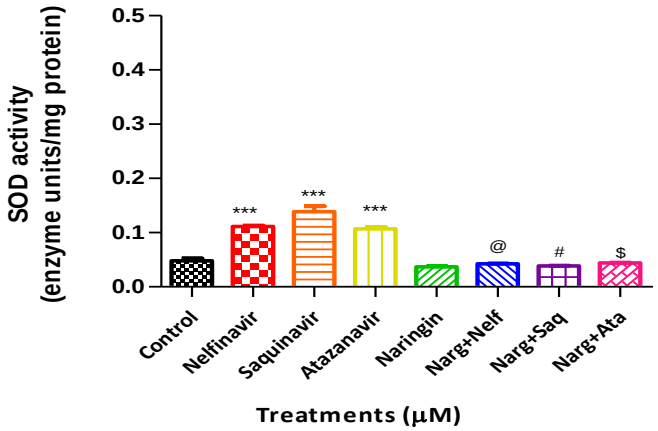

Figure 18: Superoxide dismutase activity after cells were exposed to PIs and/ or naringin (10 µM) for 24 hours at 11 mM glucose concentration. (***$p < 0.0001$ compared to controls, $^{@}p < 0.0001$ compared to nelfinavir, $^{\#}p < 0.0001$ compared to saquinavir and $^{\$}p < 0.0001$ compared to atazanavir respectively)

3.8.3 The effect of naringin on antioxidant (Glutathione)

The GSH levels in PI exposure were significantly ($p < 0.0001$) decreased compared to the untreated controls (Figure 19). However, cells exposed to combined treatment had significantly (narg+nelf; $p < 0.0001$, narg+saq; $p < 0.0001$ and narg+ata; $p < 0.0001$) higher GSH levels compared to cells treated with PIs alone. There was no significant difference in intracellular GSH levels between cells treated with naringin only and controls.

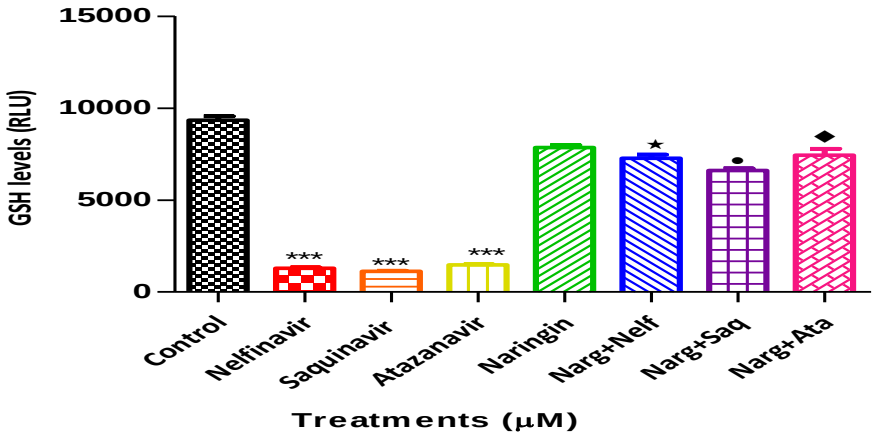

Figure 19: Glutathione levels after cells were exposed to PIs and/naringin (10 µM) for 24 hours at 11 mM glucose concentration. ***p < 0.0001 compared to controls, p< 0.0001 compared to nelfinavir, •p < 0.0001 compared to saquinavir and ♦p < 0.0001 compared to atazanavir respectively

3.8.4 The effects of naringin on ATP levels

The ATP levels in PI exposure were significantly (p < 0.0001) decreased compared to untreated controls, but were significantly higher in co-exposure (narg+nelf, narg+saq and narg+ata) compared to cells exposed to PIs alone (Figure 20). There were no significant differences in ATP levels between naringin treatment and the controls.

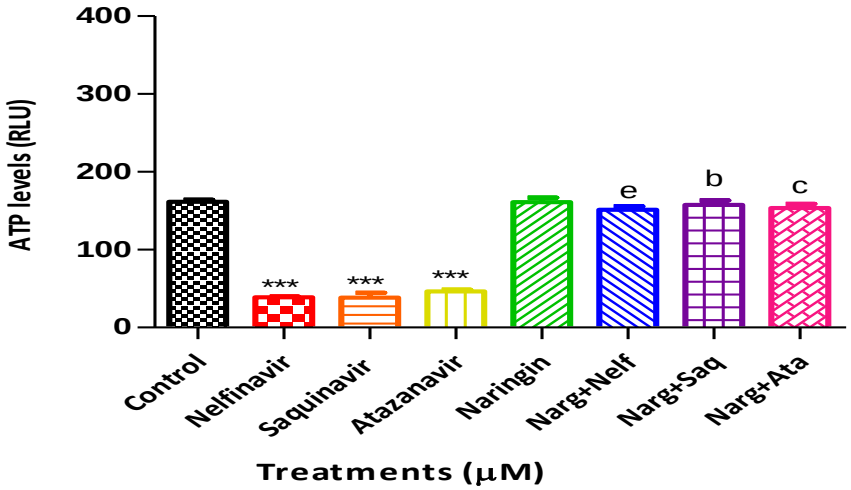

Figure 20: ATP levels after cells were exposed to PIs and/ or naringin (10 µM) for 24h at 11 mM glucose concentration. . ***$p < 0.0001$ compared to controls, $^{e}p < 0.0001$ compared to nelfinavir, $^{b}p < 0.0001$ compared to saquinavir and $^{c}p < 0.0001$ compared to atazanavir respectively

3.8.5 The effect of naringin on pro-apoptotic markers

The caspase-3 and -9 activities in PIs exposure were significantly increased ($p < 0.0001$; $p < 0.0001$) compared to the controls, respectively. However, the combined treatment of naringin and PIs significantly (narg+nelf; $p < 0.0001$, narg+saq; $p < 0.0001$ and narg+ata; $p < 0.0001$) had reduced both caspase-3 and -9 activities compared to the cells treated with PIs alone, respectively. There were no significant differences in caspase-3 and -9 respectively between naringin-treated and controls (Table 4).

Table 4: Mean values of Caspase-3 and -9 activities in RIN-5F cells treated with PIs and naringin for 24 h at 11 mM glucose concentration.

		Mean ±SD	Mean ±SD
Treatments		Caspase-3	Caspase-9
Control		317.1 ± 4.240	12570 ± 3591
	Naringin	316.4 ± 8.6	12220 ± 917.1
Nelfinavir		668.2 ± 24.0***	28190 ± 4564***
	Naringin	322.9 ± 10.8$^{\infty}$	13710 ± 1152$^{\bullet}$
Saquinavir		688.1 ± 11.3***	32070 ± 1511***
	Naringin	332.3 ± 11.3$^{\blacktriangledown}$	14070 ± 598.2$^{\blacklozenge}$
Atazanavir		671.1 ± 8.4***	28310 ± 1536***
	Naringin	312.8 ± 3.3$^{\bullet}$	11620 ± 1464^{o}

For caspase-3 ***$p < 0.0001$ compared to controls, $^{\infty}$ $p < 0.0001$ compared to nelfinavir, $^{\blacktriangledown}$ $p < 0.0001$ compared to saquinavir and $^{\bullet}$ $p < 0.0001$ compared to atazanavir respectively. RFU: Relative Fluorescence Units. For caspase-9; ***$p < 0.0001$ compared to controls, $^{\bullet}p < 0.0001$ compared to nelfinavir, $^{\blacklozenge}p < 0.0001$ compared to saquinavir and $^{o}p < 0.0001$ compared to atazanavir respectively. RLU : Relative Light Units

CHAPTER FOUR

4.1 Discussion

Chronic exposure to PIs has been linked with lipodystrophy, cardiovascular diseases, insulin resistance and type 2 diabetes (Heath et al., 2002; Souza et al., 2013; Vu et al., 2013). In the present study, we investigated whether PI-mediated β-cell dysfunction and insulin impairment is through increased oxidative stress and ATP depletion. In doing so, RIN-5F cells were exposed to different PIs (nelfinavir, saquinavir and atazanavir) and/ or glibenclamide (well-known antidiabetic drug used to increase insulin secretion in pancreatic β-cells) in the presence of varying glucose concentrations (11-25 mM), and assessed the effect of PIs on insulin secretion and oxidative stress. This study further investigated the putative protective antioxidant effects of naringin against oxidative stress induced by PIs (nelfinavir, saquinavir and atazanavir) on 11 mM glucose concentration.

Our results show that insulin secretion is glucose-dependent (Figure 10 A and B), demonstrating that pancreatic β-cells possessed normal features of glucose metabolism and insulin secretion (Patterson et al., 2014; Wallenius et al., 2002). Glucose is the primary regulator of insulin secretion in the pancreatic β-cells (Abudula et al., 2004; Guo et al., 2014; Meloni et al., 2013). The pancreatic β-cells sense an increased extracellular glucose and allow glucose to enter the cell via Glucose Transporter 2 (GLUT 2) (Guo et al., 2014; Meloni et al., 2013). Glucose is then phosphorylated by glucokinase as leading to generation of pyruvate in the cytoplasm via glycolysis pathway (Remedi and Nichols, 2009). Pyruvate enters the mitochondrion and act as a substrate for pyruvate dehydrogenase and pyruvate carboxylase leading to generation of reducing equivalents NADH and $FADH_2$ from Kreb cycle, which then activates respiratory chain for ATP synthesis (Wollheim and Maechler, 2002). This process leads to increase

intracellular ATP/ADP ratio thus triggering insulin secretion through the closure of K^+_{ATP} and open voltage-gated Ca^{2+} (Guo et al., 2014; Henquin, 2004; Wollheim and Maechler, 2002). Glibenclamide, a sulfonylurea receptor blocker, increased glucose-induced insulin secretion in the controls suggesting it role on enhancing insulin secretion (Luzi and Pozza, 1997; Patane et al., 2000).

Consequently, ATP levels were increased in a glucose-dependent manner in RIN-5F cells treated with or without PIs and/or glibenclamide for 24 hr (Figure 11 A and B). These data support the fact that insulin secretion is dependent on ATP/ADP ratio which is a normal characteristic of the response of β-cells to glucose stimulation (Henquin, 2004; Maechler and Wollheim, 2001; Wollheim and Maechler, 2002). The K^+_{ATP} channel of pancreatic β-cell is composed of four pore-forming K^+IR 6.2 subunits and the four controlling sulfonylurea receptor 1 (SUR1) together control pore permissibility (Henquin, 2004; Neye et al., 2006). The K^+IR 6.2 subunit acts as a glucose/ATP sensor (Meloni et al., 2013). ATP binds to K^+IR 6.2 closes the K^+_{ATP} channel, while binding of MgADP to SURI opens the channel (Henquin, 2004; Neye et al., 2006). This results in depolarization of cell membrane, thus opening voltage-gated Ca^{2+} (Ashcroft and Rorsman, 2013; Dart, 2012; Henquin, 2004). This leads to increase in cytosolic Ca^{2+} concentration, which will then triggers insulin release via exocytosis (Ashcroft and Rorsman, 2013; Dart, 2012; Henquin, 2004; Vlacich et al., 2010). The findings of this study are similar to those of Gu et al., (2013) who investigated the effect of ginenosine compound K (a metabolite of protopanadiol ginsenosides) with regard to the expression of GLUT 2 and intracellular ATP concentration on MIN6 pancreatic β-cells and untreated controls exhibited higher levels of both insulin and ATP in response to 3 and 30 mM glucose. Similar results were also obtained by Moynihan et al., (2005) who demonstrated that SIRT1 (enzyme that deacetylates proteins to contribute to cellular regulation) improves insulin secretion in response

to glucose and potassium chloride in β-cell-specific Sirt1-overexpressing transgenic mice. Moreover, Dufer et al (2004) evaluated the direct effect of HIV-PIs (ritonavir, nelfinavir and indinavir) with regards to stimulus-secretion coupling in β-cells. One of the observations in all treatments was an increased insulin secretion in response to 15 mM glucose compared to 3 mM. Therefore, these findings implied that RIN-5F cells used in this study retained their glucose-induced insulin secretion capacity.

However, treatment of RIN-5F cells with PIs (nelfinavir, saquinavir and atazanavir) led to reduced insulin levels in a glucose-dependent manner (Figure 10 A). This is thought to be as a result of decreased ATP concentrations due to increased production of ROS. It has been suggested that the ROS superoxide activates UCP-2, which promotes proton leakage, diminishing potential gradient and thus reducing ATP synthesis (Sakai et al., 2003). Depletion of ATP concentrations opens $K^{+}_{ATP,}$ causing partial depolarization of cell membrane, reduced cytosolic Ca^{2+} and therefore diminished insulin secretion. These findings correlated with those of Schutt et al., (2004) who found out that nelfinavir, saquinavir and ritonavir significantly impair glucose-stimulated insulin secretion accompanied by decrease in insulin-stimulated IRS-1 and Th308-Akt phosphorylation effects. Likewise, Koster et al., (2003) observed that insulin secretion from both MIN6 cell lines and rodent islets is significantly suppressed by indinavir with an IC_{50} of 1.1 and 2.1 μmol/l respectively. Therefore, our results are in agreement with other authors who report that PI treatment causes reduced insulin secretion in pancreatic β-cells. Linear regression analysis showed that decrease in insulin levels in response to nelfinavir (5-10 μM), saquinavir (5-10 μM) and atazanavir (15-25 μM) is concentration-dependent (Figure 12). However, addition of glibenclamide to PIs significantly improved insulin secretion in a glucose-dependent manner, supporting its mechanism of action by binding K^{+}_{ATP} subunit sulfonylurea

receptor 1, promoting cell membrane depolarization leading to increased Ca^{2+} influx therefore triggering insulin release by pancreatic β-cells (Figure 10 B).

In support of this, our results show a decrease in ATP concentration in response to PI and glucose (Figure 11 A), which correlates with previous findings in where insulin secretion decreased upon PI exposure. These findings are supported by those of Chandra et al., (2009) who investigated the role of PI-mediated oxidative stress in inhibiting glucose-stimulated insulin release and reported decrease in ATP levels in INS-1cells after treatment with nelfinavir for 24 hr. Glibenclamide however, increased ATP production in a glucose-dependent manner (Figure 11 B). This shows that glibenclamide increases insulin secretion which has anabolic effects on the β-cells by up-regulating antioxidant synthesis (Erejuwa et al., 2010; 2011).

This study further explored whether PI-mediated impairment of insulin secretion is through the increase oxidative stress. Oxidative stress is well-known to induce inflammation, atherosclerosis, cancer, diabetes mellitus, neurodegenerative diseases and cardiovascular disease (Sreelatha and Padma, 2011). Reactive oxygen species are enhanced to oxidize phospholipids membranes consequently leading to lipid peroxidation (Sreelatha and Padma, 2011). Polyunsaturated fatty acids (PUFAs) are mostly vulnerable to peroxidation because of the presence of double bonds between methylene-carbon (CH_2) and the reactive hydrogen (H) atom (Halliwell and Chirico, 1993). The chain reaction is initiated when free radicals react with hydrogen atoms and obstruct them from PUFAs, resulting in the formation of carbon –centered lipid radicals (Halliwell and Chirico, 1993). Lipid radicals are not stable, therefore, they reacts with oxygen (O_2) and form peroxyl radicals and hydroperoxides (Halliwell and Chirico, 1993). Peroxyl radicals are then reduced to form reactive aldehydes including malondialdehyde (MDA) and isoprostanes as by-products (Halliwell and Chirico, 1993). In this regard, our results showed

that PIs significantly increased lipid peroxidation as assessed by elevated MDA concentrations in a glucose-dependent manner (Figure 13 A). The RIN-5F cells treated with atazanavir had significantly elevated MDA concentrations compared to the controls and were also significantly lower compared to nelfinavir and saquinavir at 25 mM glucose. This implies that atazanavir produces lesser free radicals compared to both nelfinavir and saquinavir, postulating that atazanavir had lesser effects on coupling oxidative phosphorylation for ATP generation. Previous studies by Ben-Romano et al., (2006) have reported that nelfinavir and saquinavir are strongly linked with cytotoxicity in patients based on PI-therapy compared to other PIs (Kraus et al., 2013). Therefore, this finding shows that atazanavir is less likely to induce cytotoxicity compared to nelfinavir and saquinavir. Glibenclamide however, reversed MDA concentrations suggesting a role of glibenclamide in relieving oxidative stress therefore buffering the cells from oxidative damage (Figure 13 B). In addition, lipid peroxidation is known to compromise cell membranes including mitochondrial membranes which become dysfunctional (Kim et al., 2009; Sreelatha and Padma, 2011). Due to these actions, uncoupling of oxidative phosphorylation occurs, leading to increased electron leakage from the ETC and subsequent reduction of ATP production (Chandra et al., 2009; Produit-Zengaffinen et al., 2007). In several cell lines such as human myotubes, rat insulinoma cell line or vascular smooth cells, PIs have been found to induce production of ROS that is inhibited by co-exposure with the antioxidants resveratrol (Kim et al., 2009) or thymoquinone (Chandra et al., 2009) or N-acetyl cysteine (Ben-Romano et al., 2006). In the rat pancreatic insulinoma cells, a direct role of ROS in the inhibition of insulin secretion by nelfinavir is suggested because thymoquinone (a constituent of black seed oil possessed antioxidant properties) reverses the suppressive effect of nelfinavir (Chandra et al., 2009).

Superoxide is produced through the transfer of electron to oxygen molecule, and then converted to hydrogen peroxide and oxygen molecule by mitochondrial superoxide dismutase (Lenaz, 2001; Turrens, 2003). This study showed an increase in SOD activity in response to PI and glucose in a glucose dependent manner (Figure 14 A), suggesting that SOD react to accommodate excess free radicals produced. The SOD enzymes catalyses the dismutation of superoxide anion into hydrogen peroxides and oxygen molecule thus reduces the cytotoxicity (Murphy, 2009; Turrens, 2003). Glutathione scavenges hydrogen peroxide, peroxynitrite, hydroperoxides and fatty acid peroxyl radicals (Chapple et al., 2002; Marí et al., 2009). Glutathione peroxidase and glutathione-S-transferase (GST) enzymes catalyse GSH-mediated detoxification of electrophilic species (Chapple et al., 2002; Marí et al., 2009). Glutathione acts as an electron donor in a reduction reaction catalysed by GPx to detoxify peroxides (Chapple et al., 2002; Marí et al., 2009). This study shows reduced GSH levels in a glucose dependent manner but initially increased in cells that were exposed to PIs (Figure 15 A). This suggests that the combined assault of PIs and hyperglycemia initially induced antioxidant effects (by increase ROS generation) which got depleted as glucose concentrations increased. These findings are similar to those of Chandra et al., (2009) who showed the decrease insulin secretion in INS-1 cells at different concentrations of PIs (nelfinavir 5-10 μM; saquinavir 5-10 μM and atazanavir 8-20 μM) after 24 h exposure, and the treatments demonstrated the increase ROS generation and UCP2 expression, decrease GSH and ATP levels. Glibenclamide however, sustained GSH cellular content suggesting the anabolic effects of insulin which increased synthesis of inducible GSH (Figure 15 B). Altogether, our data suggests that PIs could be generating ROS which uncouple oxidative phosphorylation in the mitochondria leading to decreased inhibition of K_{ATP} pump and subsequent reduction of insulin secretion.

Excessive production of mitochondrial ROS and oxidation of mitochondrial pores lead to apoptosis (Kanno et al., 2003; Sreelatha and Padma, 2011). This stimulus for apoptosis is through the activation of Bax, a pro-apoptotic protein, which causes mitochondrial permeabilisation and the release of cytochrome C release into the mitochondrial cytoplasm (Mishra and Kumar, 2005; Park and Han, 2014). This results in the formation of apoptosome with cytochrome c, Apaf-1 and procaspase-9 (Mishra and Kumar, 2005; Park and Han, 2014). The oligomerisation of procaspase-9 in apoptosome formed results in the activation of caspase-9 which in turn activates caspase-3 (Mishra and Kumar, 2005; Park and Han, 2014). Activated caspase-3 leads to cell death characterized by chromatin condensation, nuclear fragmentation, DNA ladder and formation of apoptotic bodies (Mishra and Kumar, 2005; Park and Han, 2014). Our findings showed that PIs significantly up-regulated the activities of both caspases-3 and -9 in a glucose-dependent manner (Table 2 and 3), suggesting that RIN-5F cells undergo apoptosis after 24 h exposure to PIs and glucose. Glibenclamide however, reversed activities of both caspase-3 and -9 in a glucose-dependent manner. Correspondingly, Zang et al., (2009) reported the insulinopenia in Zucker fa/fa rats treated with PI (indinavir) for 7 weeks, suggesting chronic exposure to PI to induce β-cell dysfunction. The study was supported by increased apoptosis and reduced insulin secretion in rat insulinoma cells and human pancreatic β-cells treated with ritonavir, lopinavir, atazanavir or tipranavir for 48-96 h. In addition to study by Zang et al., (2009), chronic exposure to PIs triggers mitochondrial-associated caspase-9, causing the loss of membrane potential and promote the release of cytochrome c. In this regard, HIV-PIs induce β-cell apoptosis by triggering mitochondrial apoptosis pathway. Therefore, this study postulates that PIs impaired insulin secretion by pancreatic β-cells through increasing oxidative stress that leads to cellular damage.

Dysfunction of pancreatic β-cells is known to play a crucial role in the pathogenesis of diabetic type 2 and insulin resistance (Prentki et al., 2002; Unger, 1995). To decrease the risk of such pathological damage, it is therefore important to find the interventions that will prevent the oxidative stress and apoptosis induced by PIs so that patients acquire better prognosis. This study explored the antioxidant properties of naringin, a plant derived flavonone using 11 mM glucose concentration on RIN-5F cells exposed to different PIs; nelfinavir, saquinavir and atazanavir for 24 h. Our findings supported the beneficial effects of naringin on the PI-induced cytotoxicity. This effect of naringin is associated with its antioxidant properties, because it is postulated to have inhibited PI-induced oxidative stress. Our data show that naringin treatment exhibited a dose-dependent increase in insulin secretion ($r^2 = 0.9589$) in RIN-5F cells (Figure 16). These finding correlates with those of Ali et al (2004) who demonstrated that exogenous administration of several doses of naringin to streptozotocin-induced hyperglycemia showed decrease glucose concentration and increased insulin secretion. Addition of naringin to PIs (nelfinavir, saquinavir and atazanavir) significantly suppressed ($p < 0.0001$) PI-induced oxidative stress (Figure 17) and protected SOD expression in PIs exposure (Figure 18), suggesting the potential role of naringin as a free oxygen radical scavenger. This data is supported by previous evidence that co-treatment of naringin together with PI significantly increased ($p < 0.0001$) intracellular GSH (Figure 19) and ATP production (Figure 20), implying that naringin protect the RIN-5F cells from oxidative damage and promoting insulin secretion evidenced by increased ATP/ADP ratio. According to Amudha and Pari (2011) naringin exerts its antioxidant effects by up-regulating gene expression of SOD and GPx with subsequently scavenge ROS. Cavia-Saiz et al., (2010) postulated that the presence of hydrogen donating substituents attached to aromatic rings could enable naringin to scavenge oxidant species. Taken together, naringin treatment improved secretory responsiveness in β-cells at 11 mM glucose conditions and the mechanisms may be

involved in the protection of insulin secreting cells by reducing oxidative stress and increasing cell function.

This study further observed that naringin protect RIN-5F cells against PI-induced apoptosis. The antiapoptotic effects of naringin was due to the decrease activity of caspase-3 and -9 (Table 4) against PI-induce cellular damage and linked to its antioxidant potential. Our results are similar to previous studies that suggested to naringin have mitochondrial protectiveness against activation of caspase-3 and -9; it decreases expression of Bax, p53 protein and cleavages of caspase-3, and increases expression of Bcl2 (Sahu et al., 2014). Hak-Jae at al., (2009) demonstrated that naringin prevented rotenone-induced phosphorylation of JNK and p38; therefore preventing changes in Bcl2 and associated with Bax expression levels in human SH-SY5Y cells. In addition, Hak-Jae et al., (2009) further provided more evidence with regards to decrease in apoptosis by naringin in human SH-SY5Y cells by it preventing cleavages of caspase-9, poly (ADP-ribose) polymerase (PARP; a biochemical hallmark of apoptosis) and caspase-3 and decrease enzyme activity of caspase-3. Consequently Chen et al., (2014), demonstrated that naringin protects cardiac H9c2 cells-induced hyperglycemia from apoptosis by inhibiting stimulation of MAPK, especially JNK, ERK1/2 and p38 MAPK. C-Jun NH_2 terminal kinase is known to release apoptogenic factors cytochrome c and smac/DIABLO to initiate apoptosis whereas p38 MAPK is involved in the phosphorylation of Bcl2 and triggering mitochondrial apoptotic pathway (Chen et al., 2014). Our data clearly suggest that naringin prevent apoptosis in RIN-5F cells under 11 mM glucose concentration and the mechanisms involved may be though reduction of oxidative stress that is known to induce cell death, therefore increasing cell survival.

CHAPTER FIVE

5.0 Conclusions

Metabolic syndrome in HIV patients receiving PI-based therapy has been becomes a major concern worldwide. Protease inhibitors (PIs) were shown to induce β-cell dysfunction and impair insulin secretion by increasing oxidative stress and ATP depletion. Dysfunction or reduced numbers of pancreatic β-cells are the influential factors in the development of type 2 diabetes and insulin resistance. Therefore, this emphasizes the need for the development of cheap and safer therapies such a naturally occurring flavonone, naringin to improve longevity brought by antiretroviral regimen.

Our data showed that HIV-PIs inhibit glucose-induce insulin secretion in pancreatic β-cells. The effect is mediated through increased oxidative stress, decrease ATP and antioxidant (GSH) mechanisms. Moreover, our study showed that naringin ameliorated PIs-induced impairment of β-cell dysfunction at 11 mM glucose concentration by reducing oxidative stress and preserved pancreatic β-cell integrity. These findings therefore suggest that naringin may be considered as a therapeutic agent in the management of PI-associated metabolic syndrome with respect to pancreatic β-cell dysfunction.

However, it is recommended that the role of naringin at different concentrations of HIV-PIs as well as of glucose should be considered in further/subsequent studies. The cytological analysis of the cultured cells under various concentrations of HIV-PIs/ naringin should be done to ascertain if there are any mitochondrial structural changes. Concentration levels of Ca^{2+} ions should be determined at various HIV-PIs/ naringin treatment levels. Lastly, the expression of uncoupling protein 2 should be determined at various HIV/PIs/ naringin concentration levels.

Furthermore, this study recommends that studies be carried out to ascertain the effects of naringin *in vivo* and isolated pancreatic β-cells with respect to oxidative stress, anti-oxidant capacity, insulin secretion and apoptosis. This study also recommends that studies be carried out to ascertain the effects of naringin in different pancreatic β-cell lines in a glucose dependent environment for the purpose of generating baseline data for the respective cell-line.

REFERENCES

Aberg JA (2009) Lipid management in patients who have HIV and are receiving HIV therapy. Endocrinol Metab Clin North Am 38:207-222.

Abudula R, Jeppesen PB, Rolfsen SE, Xiao J and Hermansen K (2004) Rebaudioside A potently stimulates insulin secretion from isolated mouse islets: studies on the dose-, glucose-, and calcium-dependency. Metabolism: clinical and experimental 53:1378-1381.

Ahmadi R, Pishghadam S, Mollaamine F and Zand Monfared MR (2013) Comparing the effects of ginger and glibenclamide on dihydroxybenzoic metabolites produced in stz-induced diabetic rats. International journal of endocrinology and metabolism 11:e10266.

Alberti KG, Zimmet P and Shaw J (2005) The metabolic syndrome--a new worldwide definition. Lancet 366:1059-1062.

Amudha K and Pari L (2011) Beneficial role of naringin, a flavanoid on nickel induced nephrotoxicity in rats. Chemico-biological interactions 193:57-64.

Anuurad E, Bremer A and Berglund L (2010) HIV protease inhibitors and obesity. Curr Opin Endocrinol Diabetes Obes 17:478-485.

Apostolova N, Blas-Garcia A and Esplugues JV (2011) Mitochondrial interference by anti-HIV drugs: mechanisms beyond Pol-gamma inhibition. Trends Pharmacol Sci 32:715-725.

Ashcroft FM and Rorsman P (2013) KATP channels and islet hormone secretion: new insights and controversies. Nat Rev Endocrinol 9:660-669.

Barbaro G (2006) Metabolic and cardiovascular complications of highly active antiretroviral therapy for HIV infection. Current HIV research 4:79-85.

Bastard JP, Maachi M, Van Nhieu JT, Jardel C, Bruckert E, Grimaldi A, Robert JJ, Capeau J and Hainque B (2002) Adipose tissue IL-6 content correlates with resistance to insulin activation of glucose uptake both in vivo and in vitro. The Journal of clinical endocrinology and metabolism 87:2084-2089.

Bekker LG, Venter F, Cohen K, Goemare E, Van Cutsem G, Boulle A and Wood R (2014) Provision of antiretroviral therapy in South Africa: the nuts and bolts. Antiviral therapy 19 Suppl 3:105-116.

Ben-Romano R, Rudich A, Etzion S, Potashnik R, Kagan E, Greenbaum U and Bashan N (2006) Nelfinavir induces adipocyte insulin resistance through the induction of oxidative stress: differential protective effect of antioxidant agents. Antiviral therapy 11:1051-1060.

Beyrer C and Abdool Karim Q (2013) The changing epidemiology of HIV in 2013. Current opinion in HIV and AIDS 8:306-310.

Bonnet E (2010) New and emerging agents in the management of lipodystrophy in HIV-infected patients. HIV AIDS (Auckl) 2:167-178.

Bradford MM (1976) A rapid and sensitive method for the quantitation of microgram quantities of protein utilizing the principle of protein-dye binding. Analytical biochemistry 72:248-254.

Brown JE, Thomas S, Digby JE and Dunmore SJ (2002) Glucose induces and leptin decreases expression of uncoupling protein-2 mRNA in human islets. FEBS letters 513:189-192.

Cahn P, Leite O, Rosales A, Cabello R, Alvarez CA, Seas C, Carcamo C, Cure-Bolt N, L'Italien GP, Mantilla P, Deibis L, Zala C and Suffert T (2010) Metabolic profile and cardiovascular risk factors among Latin American HIV-infected patients receiving HAART. The Brazilian

journal of infectious diseases : an official publication of the Brazilian Society of Infectious Diseases 14:158-166.

Carper MJ, Cade WT, Cam M, Zhang S, Shalev A, Yarasheski KE and Ramanadham S (2008) HIV-protease inhibitors induce expression of suppressor of cytokine signaling-1 in insulin-sensitive tissues and promote insulin resistance and type 2 diabetes mellitus. American journal of physiology Endocrinology and metabolism 294:E558-567.

Carr A (2000) HIV protease inhibitor-related lipodystrophy syndrome. Clin Infect Dis 30 Suppl 2:S135-142.

Carr A and Cooper DA (2000) Adverse effects of antiretroviral therapy. Lancet 356:1423-1430.

Carr A, Samaras K, Burton S, Law M, Freund J, Chisholm DJ and Cooper DA (1998) A syndrome of peripheral lipodystrophy, hyperlipidaemia and insulin resistance in patients receiving HIV protease inhibitors. AIDS (London, England) 12:F51-58.

Castilla J, Del Romero J, Hernando V, Marincovich B, Garcia S and Rodriguez C (2005) Effectiveness of highly active antiretroviral therapy in reducing heterosexual transmission of HIV. Journal of acquired immune deficiency syndromes (1999) 40:96-101.

Cavia-Saiz M, Busto MD, Pilar-Izquierdo MC, Ortega N, Perez-Mateos M and Muniz P (2010) Antioxidant properties, radical scavenging activity and biomolecule protection capacity of flavonoid naringenin and its glycoside naringin: a comparative study. Journal of the science of food and agriculture 90:1238-1244.

Chandra S, Mondal D and Agrawal KC (2009) HIV-1 protease inhibitor induced oxidative stress suppresses glucose stimulated insulin release: protection with thymoquinone. Experimental biology and medicine (Maywood, NJ) 234:442-453.

Chapple ILC, Brock G, Eftimiadi C and Matthews JB (2002) Glutathione in gingival crevicular fluid and its relation to local antioxidant capacity in periodontal health and disease. Molecular Pathology 55:367-373.

Chen J, Guo R, Yan H, Tian L, You Q, Li S, Huang R and Wu K (2014) Naringin inhibits ROS-activated MAPK pathway in high glucose-induced injuries in H9c2 cardiac cells. Basic & clinical pharmacology & toxicology 114:293-304.

Clinicians Society SH (2013) Fixed-dose combination for adults accessing antiretroviral therapy.

Crawford KW, Li X, Xu X, Abraham AG, Dobs AS, Margolick JB, Palella FJ, Kingsley LA, Witt MD and Brown TT (2013) Lipodystrophy and inflammation predict later grip strength in HIV-infected men: the MACS Body Composition substudy. AIDS Res Hum Retroviruses 29:1138-1145.

Dart C (2012) Selective block of K(ATP) channels: why the anti-diabetic sulphonylureas and rosiglitazone have more in common than we thought. British Journal of Pharmacology 167:23-25.

Dau B and Holodniy M (2008) The Relationship Between HIV Infection and Cardiovascular Disease. Curr Cardiol Rev 4:203-218.

Domingo P, Vidal F, Domingo JC, Veloso S, Sambeat MA, Torres F, Sirvent JJ, Vendrell J, Matias-Guiu X and Richart C (2005) Tumour necrosis factor alpha in fat redistribution syndromes associated with combination antiretroviral therapy in HIV-1-infected patients: potential role in subcutaneous adipocyte apoptosis. Eur J Clin Invest 35:771-780.

Echtay KS, Roussel D, St-Pierre J, Jekabsons MB, Cadenas S, Stuart JA, Harper JA, Roebuck SJ, Morrison A, Pickering S, Clapham JC and Brand MD (2002) Superoxide activates mitochondrial uncoupling proteins. Nature 415:96-99.

Erejuwa OO, Sulaiman SA, Wahab MS, Salam SK, Salleh MS and Gurtu S (2010) Antioxidant protective effect of glibenclamide and metformin in combination with honey in pancreas of streptozotocin-induced diabetic rats. Int J Mol Sci 11:2056-2066.

Erejuwa OO, Sulaiman SA, Wahab MS, Salam SK, Salleh MS and Gurtu S (2011) Comparison of antioxidant effects of honey, glibenclamide, metformin, and their combinations in the kidneys of streptozotocin-induced diabetic rats. Int J Mol Sci 12:829-843.

Estrada V and Portilla J (2011) Dyslipidemia related to antiretroviral therapy. AIDS reviews 13:49-56.

Feeney ER and Mallon PW (2011) HIV and HAART-Associated Dyslipidemia. Open Cardiovasc Med J 5:49-63.

Flint OP, Noor MA, Hruz PW, Hylemon PB, Yarasheski K, Kotler DP, Parker RA and Bellamine A (2009) The role of protease inhibitors in the pathogenesis of HIV-associated lipodystrophy: cellular mechanisms and clinical implications. Toxicol Pathol 37:65-77.

Frederich RC, Hamann A, Anderson S, Lollmann B, Lowell BB and Flier JS (1995) Leptin levels reflect body lipid content in mice: evidence for diet-induced resistance to leptin action. Nature medicine 1:1311-1314.

Friedman JM (2009) Leptin at 14 y of age: an ongoing story. The American journal of clinical nutrition 89:973S-979S.

Fruebis J, Tsao TS, Javorschi S, Ebbets-Reed D, Erickson MR, Yen FT, Bihain BE and Lodish HF (2001) Proteolytic cleavage product of 30-kDa adipocyte complement-related protein increases fatty acid oxidation in muscle and causes weight loss in mice. Proc Natl Acad Sci U S A 98:2005-2010.

Gandhi M and Gandhi RT (2014) Single-pill combination regimens for treatment of HIV-1 infection. The New England journal of medicine 371:248-259.

Gayoso-Diz P, Otero-González A, Rodriguez-Alvarez M, Gude F, García F, De Francisco A and Quintela A (2013) Insulin resistance (HOMA-IR) cut-off values and the metabolic syndrome in a general adult population: effect of gender and age: EPIRCE cross-sectional study. BMC Endocr Disord 13:1-10.

Goillot E, Raingeaud J, Ranger A, Tepper RI, Davis RJ, Harlow E and Sanchez I (1997) Mitogen-activated protein kinase-mediated Fas apoptotic signaling pathway. Proc Natl Acad Sci U S A 94:3302-3307.

Gopinath K and Sudhandiran G (2012) Naringin modulates oxidative stress and inflammation in 3-nitropropionic acid-induced neurodegeneration through the activation of nuclear factor-erythroid 2-related factor-2 signalling pathway. Neuroscience 227:134-143.

Guaraldi G, Orlando G, De Fazio D, De Lorenzi I, Rottino A, De Santis G, Pedone A, Spaggiari A, Baccarani A, Borghi V and Esposito R (2005) Comparison of three different interventions for the correction of HIV-associated facial lipoatrophy: a prospective study. Antiviral therapy 10:753-759.

Guo JH, Chen H, Ruan YC, Zhang XL, Zhang XH, Fok KL, Tsang LL, Yu MK, Huang WQ, Sun X, Chung YW, Jiang X, Sohma Y and Chan HC (2014) Glucose-induced electrical

activities and insulin secretion in pancreatic islet β-cells are modulated by CFTR. Nat Commun 5.

Halliwell B and Chirico S (1993) Lipid peroxidation: its mechanism, measurement, and significance. The American journal of clinical nutrition 57:715S-724S; discussion 724S-725S.

Heath KV, Hogg RS, Singer J, Chan KJ, O'Shaughnessy MV and Montaner JS (2002) Antiretroviral treatment patterns and incident HIV-associated morphologic and lipid abnormalities in a population-based chort. Journal of acquired immune deficiency syndromes (1999) 30:440-447.

Henquin JC (2004) Pathways in beta-cell stimulus-secretion coupling as targets for therapeutic insulin secretagogues. Diabetes 53 Suppl 3:S48-58.

Hruz PW, Murata H and Mueckler M (2001) Adverse metabolic consequences of HIV protease inhibitor therapy: the search for a central mechanism. American journal of physiology Endocrinology and metabolism 280:E549-553.

Hui DY (2003) Effects of HIV protease inhibitor therapy on lipid metabolism. Progress in lipid research 42:81-92.

James DE, Strube M and Mueckler M (1989) Molecular cloning and characterization of an insulin-regulatable glucose transporter. Nature 338:83-87.

James J, Carruthers A and Carruthers J (2002) HIV-associated facial lipoatrophy. Dermatol Surg 28:979-986.

Kalra S, Kalra B, Agrawal N and Unnikrishnan A (2011) Understanding diabetes in patients with HIV/AIDS. Diabetology & metabolic syndrome 3:2.

Kanno S, Shouji A, Asou K and Ishikawa M (2003) Effects of naringin on hydrogen peroxide-induced cytotoxicity and apoptosis in P388 cells. Journal of pharmacological sciences 92:166-170.

Kim HJ, Song JY, Park HJ, Park HK, Yun DH and Chung JH (2009) Naringin Protects against Rotenone-induced Apoptosis in Human Neuroblastoma SH-SY5Y Cells. The Korean journal of physiology & pharmacology : official journal of the Korean Physiological Society and the Korean Society of Pharmacology 13:281-285.

Kim JA, Wei Y and Sowers JR (2008) Role of mitochondrial dysfunction in insulin resistance. Circulation research 102:401-414.

Kis O, Robillard K, Chan GN and Bendayan R (2010) The complexities of antiretroviral drug-drug interactions: role of ABC and SLC transporters. Trends Pharmacol Sci 31:22-35.

Koster JC, Remedi MS, Qiu H, Nichols CG and Hruz PW (2003) HIV protease inhibitors acutely impair glucose-stimulated insulin release. Diabetes 52:1695-1700.

Kraus M, Bader J, Overkleeft H and Driessen C (2013) Nelfinavir augments proteasome inhibition by bortezomib in myeloma cells and overcomes bortezomib and carfilzomib resistance. Blood Cancer Journal 3:e103.

Krauss S, Zhang CY, Scorrano L, Dalgaard LT, St-Pierre J, Grey ST and Lowell BB (2003) Superoxide-mediated activation of uncoupling protein 2 causes pancreatic beta cell dysfunction. The Journal of clinical investigation 112:1831-1842.

Krude H, Biebermann H, Luck W, Horn R, Brabant G and Gruters A (1998) Severe early-onset obesity, adrenal insufficiency and red hair pigmentation caused by POMC mutations in humans. Nature genetics 19:155-157.

Lenaz G (2001) The mitochondrial production of reactive oxygen species: mechanisms and implications in human pathology. IUBMB life 52:159-164.

Leow MK, Addy CL and Mantzoros CS (2003) Clinical review 159: Human immunodeficiency virus/highly active antiretroviral therapy-associated metabolic syndrome: clinical presentation, pathophysiology, and therapeutic strategies. The Journal of clinical endocrinology and metabolism 88:1961-1976.

Leung VL and Glesby MJ (2011) Pathogenesis and treatment of HIV lipohypertrophy. Curr Opin Infect Dis 24:43-49.

Loonam CR and Mullen A (2012) Nutrition and the HIV-associated lipodystrophy syndrome. Nutr Res Rev 25:267-287.

Lowell BB and Shulman GI (2005) Mitochondrial dysfunction and type 2 diabetes. Science (New York, NY) 307:384-387.

Luzi L and Pozza G (1997) Glibenclamide: an old drug with a novel mechanism of action? Acta diabetologica 34:239-244

Maartens G, Celum C and Lewin SR (2014) HIV infection: epidemiology, pathogenesis, treatment, and prevention. The Lancet 384:258-271.

MacDermott RP (1996) Alterations of the mucosal immune system in inflammatory bowel disease. Journal of gastroenterology 31:907-916.

Maechler P and Wollheim CB (2001) Mitochondrial function in normal and diabetic beta-cells. Nature 414:807-812.

Marí M, Morales A, Colell A, García-Ruiz C and Fernández-Checa JC (2009) Mitochondrial Glutathione, a Key Survival Antioxidant. Antioxidants & Redox Signaling 11:2685-2700.

Matough FA, Budin SB, Hamid ZA, Alwahaibi N and Mohamed J (2012) The Role of Oxidative Stress and Antioxidants in Diabetic Complications. Sultan Qaboos University Medical Journal 12:5-18.

Meloni AR, DeYoung MB, Lowe C and Parkes DG (2013) GLP-1 receptor activated insulin secretion from pancreatic beta-cells: mechanism and glucose dependence. Diabetes, obesity & metabolism 15:15-27.

Mencarelli A, Francisci D, Renga B, D'Amore C, Cipriani S, Basile F, Schiaroli E, Baldelli F and Fiorucci S (2012) Ritonavir-induced lipoatrophy and dyslipidaemia is reversed by the anti-inflammatory drug leflunomide in a PPAR-gamma-dependent manner. Antiviral therapy 17:669-678.

Mishra NC and Kumar S (2005) Apoptosis: a mitochondrial perspective on cell death. Indian journal of experimental biology 43:25-34.

Montague CT, Farooqi IS, Whitehead JP, Soos MA, Rau H, Wareham NJ, Sewter CP, Digby JE, Mohammed SN, Hurst JA, Cheetham CH, Earley AR, Barnett AH, Prins JB and O'Rahilly S (1997) Congenital leptin deficiency is associated with severe early-onset obesity in humans. Nature 387:903-908.

Murphy MP (2009) How mitochondria produce reactive oxygen species. The Biochemical journal 417:1-13.

Neye Y, Dufer M, Drews G and Krippeit-Drews P (2006) HIV protease inhibitors: suppression of insulin secretion by inhibition of voltage-dependent K+ currents and anion currents. The Journal of pharmacology and experimental therapeutics 316:106-112.

Palios J, Kadoglou NP and Lampropoulos S (2012) The pathophysiology of HIV-/HAART-related metabolic syndrome leading to cardiovascular disorders: the emerging role of adipokines. Exp Diabetes Res 2012:103063.

Park MH and Han JS (2014) Padina arborescens extract protects high glucose-induced apoptosis in pancreatic beta cells by reducing oxidative stress. Nutrition research and practice 8:494-500.

Patane G, Piro S, Anello M, Rabuazzo AM, Vigneri R and Purrello F (2000) Exposure to glibenclamide increases rat beta cells sensitivity to glucose. Br J Pharmacol 129:887-892.

Patterson JN, Cousteils K, Lou JW, Manning Fox JE, MacDonald PE and Joseph JW (2014) Mitochondrial metabolism of pyruvate is essential for regulating glucose-stimulated insulin secretion. The Journal of biological chemistry 289:13335-13346.

Prentki M, Joly E, El-Assaad W and Roduit R (2002) Malonyl-CoA signaling, lipid partitioning, and glucolipotoxicity: role in beta-cell adaptation and failure in the etiology of diabetes. Diabetes 51 Suppl 3:S405-413.

Produit-Zengaffinen N, Davis-Lameloise N, Perreten H, Becard D, Gjinovci A, Keller PA, Wollheim CB, Herrera P, Muzzin P and Assimacopoulos-Jeannet F (2007) Increasing uncoupling protein-2 in pancreatic beta cells does not alter glucose-induced insulin secretion but decreases production of reactive oxygen species. Diabetologia 50:84-93.

Qatanani M and Lazar MA (2007) Mechanisms of obesity-associated insulin resistance: many choices on the menu. Genes & development 21:1443-1455.

Rajadurai M and Stanely Mainzen Prince P (2006) Preventive effect of naringin on lipid peroxides and antioxidants in isoproterenol-induced cardiotoxicity in Wistar rats: biochemical and histopathological evidences. Toxicology 228:259-268.

Rankinen T, Zuberi A, Chagnon YC, Weisnagel SJ, Argyropoulos G, Walts B, Perusse L and Bouchard C (2006) The human obesity gene map: the 2005 update. Obesity (Silver Spring, Md) 14:529-644.

Remedi MS and Nichols CG (2009) Hyperinsulinism and Diabetes: Genetic Dissection of β Cell Metabolism-Excitation Coupling in Mice. Cell Metabolism 10:442-453.

Rieusset J, Bouzakri K, Chevillotte E, Ricard N, Jacquet D, Bastard JP, Laville M and Vidal H (2004) Suppressor of cytokine signaling 3 expression and insulin resistance in skeletal muscle of obese and type 2 diabetic patients. Diabetes 53:2232-2241.

Robertson R, Zhou H, Zhang T and Harmon JS (2007) Chronic oxidative stress as a mechanism for glucose toxicity of the beta cell in type 2 diabetes. Cell biochemistry and biophysics 48:139-146.

Rudich A, Ben-Romano R, Etzion S and Bashan N (2005) Cellular mechanisms of insulin resistance, lipodystrophy and atherosclerosis induced by HIV protease inhibitors. Acta Physiol Scand 183:75-88.

Rudich A, Vanounou S, Riesenberg K, Porat M, Tirosh A, Harman-Boehm I, Greenberg AS, Schlaeffer F and Bashan N (2001) The HIV protease inhibitor nelfinavir induces insulin resistance and increases basal lipolysis in 3T3-L1 adipocytes. Diabetes 50:1425-1431.

Sahu BD, Tatireddy S, Koneru M, Borkar RM, Kumar JM, Kuncha M, Srinivas R, Shyam Sunder R and Sistla R (2014) Naringin ameliorates gentamicin-induced nephrotoxicity and associated mitochondrial dysfunction, apoptosis and inflammation in rats: possible mechanism of nephroprotection. Toxicology and applied pharmacology 277:8-20.

Sakai K, Matsumoto K, Nishikawa T, Suefuji M, Nakamaru K, Hirashima Y, Kawashima J, Shirotani T, Ichinose K, Brownlee M and Araki E (2003) Mitochondrial reactive oxygen

species reduce insulin secretion by pancreatic beta-cells. Biochemical and biophysical research communications 300:216-222.

Samaras K, Wand H, Law M, Emery S, Cooper D and Carr A (2007) Prevalence of metabolic syndrome in HIV-infected patients receiving highly active antiretroviral therapy using International Diabetes Foundation and Adult Treatment Panel III criteria: associations with insulin resistance, disturbed body fat compartmentalization, elevated C-reactive protein, and [corrected] hypoadiponectinemia. Diabetes care 30:113-119.

Samaras K, Wand H, Law M, Emery S, Cooper DA and Carr A (2009) Dietary intake in HIV-infected men with lipodystrophy: relationships with body composition, visceral fat, lipid, glucose and adipokine metabolism. Curr HIV Res 7:454-461.

Saves M, Raffi F, Capeau J, Rozenbaum W, Ragnaud JM, Perronne C, Basdevant A, Leport C and Chene G (2002) Factors related to lipodystrophy and metabolic alterations in patients with human immunodeficiency virus infection receiving highly active antiretroviral therapy. Clinical infectious diseases : an official publication of the Infectious Diseases Society of America 34:1396-1405.

Savini I, Catani MV, Evangelista D, Gasperi V and Avigliano L (2013) Obesity-Associated Oxidative Stress: Strategies Finalized to Improve Redox State. International Journal of Molecular Sciences 14:10497-10538.

Schutt M, Zhou J, Meier M and Klein HH (2004) Long-term effects of HIV-1 protease inhibitors on insulin secretion and insulin signaling in INS-1 beta cells. The Journal of endocrinology 183:445-454.

Shiozaki EN, Chai J and Shi Y (2002) Oligomerization and activation of caspase-9, induced by Apaf-1 CARD. Proceedings of the National Academy of Sciences 99:4197-4202.

Singhania R and Kotler DP (2011) Lipodystrophy in HIV patients: its challenges and management approaches. HIV AIDS (Auckl) 3:135-143.

Souza SJ, Luzia LA, Santos SS and Rondó PHC (2013) Lipid profile of HIV-infected patients in relation to antiretroviral therapy: a review. Revista da Associação Médica Brasileira 59:186-198.

Sreelatha S and Padma PR (2011) Modulatory effects of Moringa oleifera extracts against hydrogen peroxide-induced cytotoxicity and oxidative damage. Human & experimental toxicology 30:1359-1368.

Thangavel P, Muthu R and Vaiyapuri M (2012) Antioxidant potential of naringin – a dietary flavonoid – in N-Nitrosodiethylamine induced rat liver carcinogenesis. Biomedicine & Preventive Nutrition 2:193-202.

Tsiodras S, Perelas A, Wanke C and Mantzoros CS (2010) The HIV-1/HAART associated metabolic syndrome - novel adipokines, molecular associations and therapeutic implications. J Infect 61:101-113.

Turrens JF (2003) Mitochondrial formation of reactive oxygen species. The Journal of physiology 552:335-344.

Unger RH (1995) Lipotoxicity in the pathogenesis of obesity-dependent NIDDM. Genetic and clinical implications. Diabetes 44:863-870.

Vlacich G, Nawijn MC, Webb GC and Steiner DF (2010) Pim3 negatively regulates glucose-stimulated insulin secretion. Islets 2:308-317.

Vu CN, Ruiz-Esponda R, Yang E, Chang E, Gillard B, Pownall HJ, Hoogeveen RC, Coraza I and Balasubramanyam A (2013) Altered relationship of plasma triglycerides to HDL

cholesterol in patients with HIV/HAART-associated dyslipidemia: Further evidence for a unique form of Metabolic Syndrome in HIV patients. Metabolism: clinical and experimental 62:1014-1020.

Wada T and Penninger JM (2004) Mitogen-activated protein kinases in apoptosis regulation. Oncogene 23:2838-2849.

Wallenius V, Wallenius K, Ahren B, Rudling M, Carlsten H, Dickson SL, Ohlsson C and Jansson JO (2002) Interleukin-6-deficient mice develop mature-onset obesity. Nature medicine 8:75-79.

Waters L and Nelson M (2007) Long-term complications of antiretroviral therapy: lipoatrophy. Int J Clin Pract 61:999-1014.

Woerle HJ, Mariuz PR, Meyer C, Reichman RC, Popa EM, Dostou JM, Welle SL and Gerich JE (2003) Mechanisms for the deterioration in glucose tolerance associated with HIV protease inhibitor regimens. Diabetes 52:918-925.

Wollheim CB and Maechler P (2002) Beta-cell mitochondria and insulin secretion: messenger role of nucleotides and metabolites. Diabetes 51 Suppl 1:S37-42.

Yeo GS, Farooqi IS, Aminian S, Halsall DJ, Stanhope RG and O'Rahilly S (1998) A frameshift mutation in MC4R associated with dominantly inherited human obesity. Nature genetics 20:111-112.

Zhang HH, Halbleib M, Ahmad F, Manganiello VC and Greenberg AS (2002) Tumor necrosis factor-alpha stimulates lipolysis in differentiated human adipocytes through activation of extracellular signal-related kinase and elevation of intracellular cAMP. Diabetes 51:2929-2935.

Appendix A

Insulin ELISA

Table A and B: Glucose-induced insulin secretion in cells that were treated with (A) PIs and/or (B) glibenclamide

A

Glucose (mM)	Control		Nelfinavir		Saquinavir		Atazanavir	
11	3.2930	2.6770	1.165	1.115	1.224	1.295	1.346	1.137
15	3.1350	3.5900	1.880	1.780	1.934	2.040	2.011	1.890
20	4.4500	4.2010	2.452	2.615	2.580	2.690	2.434	2.363
25	5.0050	5.1130	3.490	3.370	3.514	3.650	3.685	3.480

B

Glucose (mM)	Glibenclamide		Nelf+Glibn		Saq+Glibn		Ata+Glibn	
11	4.044	4.091	1.864	1.523	1.8750	1.8400	1.8450	1.9130
15	4.890	4.750	2.870	2.984	2.8550	2.7600	2.6500	2.7400
20	6.610	6.550	3.383	3.465	3.4200	3.6350	3.3100	3.4220
25	8.010	8.160	4.550	4.340	4.4600	4.5500	4.1110	4.3250

ATP assay

Table A and B: ATP productions after cells were treated with (A) PIs and/or (B) glibenclamide at different concentrations of glucose.

A

Glucose (mM)	Control			Nelfinavir			Saquinavir			Atazanavir		
11	162.212	166.030	156.483	40.05	37.924	39.261	47.661	26.469	41.170	49.570	47.852	42.125
15	262.120	266.549	244.756	80.123	64.810	80.421	70.513	59.820	75.010	90.540	88.615	84.125
20	508.100	515.230	512.115	109.134	151.089	116.101	108.165	121.175	117.641	151.089	161.176	121.195
25	809.100	789.036	816.450	220.128	225.059	225.056	216.561	205.456	213.075	245.701	265.147	278.265

B

Glucose (mM)	Glibenclamide			Nelf+Glibn			Saq+Glibn			Ata+Glibn		
11	280.011	279.890	285.001	108.755	118.165	103.392	105.028	89.119	109.209	101.665	118.574	97.847
15	405.962	415.040	409.222	148.046	144.258	180.409	133.831	158.019	166.963	184.650	175.280	165.684
20	650.786	659.165	647.952	405.153	418.222	416.236	390.450	385.162	365.124	415.365	416.023	420.125
25	865.984	871.614	889.001	606.498	616.579	610.956	589.563	572.146	601.000	615.896	625.357	625.364

Insulin ELISA

Linear regression analysis of concentration-depend inhibition of insulin secretion in RIN-5F cultured cells.

Insulin secretion (µg/L)	**Nelfinavir**		**Saquinavir**		**Atazanavir**	
0.0	1.473922	1.352518			1.162825	1.079360
2.5	1.291816	1.109710	1.170412	1.003482		
5.0	0.798613	0.6544458	0.4951031	0.4647521	0.9048414	1.155237
7.5	0.2067688	0.2674707	0.4192257	0.3812869		
10.0	0.1688301	0.1233036	0.2067688	0.320585	0.7530864	0.7379109
15.0	0.01783392	0.05729019	0.1840055	0.1308913	0.5861561	0.4192257
20.0				0.0550138	0.2067688	0.1688301
25.0			0.0594874	8		0.0626016
					0.1233036	1

Lipid peroxidation

Table A and B: TBARS assay measured as MDA concentrations after cells were treated with (A) PIs and/or (B) glibenclamide at different concentrations of glucose.

A

Glucose (mM)	Control			Nelfinavir			Saquinavir			Atazanavir		
11	0.025	0.023	0.023	0.278	0.380	0.378	0.358	0.373	0.283	0.275	0.260	0.262
15	0.030	0.033	0.041	0.340	0.360	0.360	0.389	0.375	0.315	0.310	0.314	0.320
20	0.765	0.780	1.090	1.020	1.085	1.090	1.163	1.129	0.950	0.932	0.940	0.960
25	2.580	2.660	2.590	3.390	3.411	3.421	3.401	3.375	3.391	2.900	2.920	2.750

B

Glucose (mM)	Glibenclamide			Nelf+Glibn			Saq+Glibn			Ata+Glibn		
11	0.0250	0.0210	0.0190	0.106	0.072	0.090	0.072	0.075	0.084	0.040	0.065	0.055
15	0.0220	0.0350	0.0260	0.206	0.144	0.188	0.144	0.140	0.165	0.080	0.135	0.110
20	0.0310	0.0350	0.0290	0.616	0.432	0.564	0.430	0.440	0.506	0.428	0.436	0.425
25	0.0290	0.0400	0.0330	2.550	2.720	2.701	2.270	2.760	2.280	1.890	1.980	1.880

Table A and B: SOD activity after cells were exposed with (A) PIs and/or (B) glibenclamide at different concentrations of glucose

A

Glucose (mM)	Control			Nelfinavir			Saquinavir			Atazanavir		
11	0.048	0.040	0.056	0.115	0.109	0.110	0.158	0.130	0.128	0.108	0.112	0.100
15	0.096	0.090	0.110	0.230	0.228	0.220	0.316	0.270	0.256	0.226	0.235	0.265
20	0.288	0.276	0.330	0.690	0.680	0.664	0.715	0.720	0.723	0.678	0.716	0.700
25	1.864	1.810	1.790	2.070	2.052	1.980	2.130	2.160	2.175	2.034	2.111	2.136

B

Glucose (mM)	Glibenclamide			Nelf+Glibn			Saq+Glibn			Ata+Glibn		
11	0.098	0.102	0.101	0.077	0.055	0.055	0.065	0.053	0.049	0.070	0.040	0.041
15	0.204	0.201	0.198	0.140	0.125	0.130	0.130	0.106	0.098	0.140	0.160	0.168
20	0.615	0.613	0.598	0.423	0.375	0.395	0.390	0.382	0.285	0.387	0.401	0.419
25	1.861	1.761	1.858	1.160	1.075	1.090	1.170	0.989	0.885	1.244	1.215	1.235

Glutathione (GSH) assay

Table A and B: Glutathione levels after cells were exposed with (A) PIs and/or (B) glibenclamide at different concentrations of glucose.

A

Glucose (mM)	Control			Nelfinavir			Saquinavir			Atazanavir		
11	9501.00	9616.12	8896.36	210.45	1281.59	1381.99	1152.4	1071.1	1159.6	1538.23	1420.92	1454.55
15	7818.00	7734.01	7832.12	4227.74	4112.84	4051.52	4085.9	3763.4	4001.8	4365.24	4296.62	4458.90
20	5252.13	5193.43	5908.61	3182.41	3161.14	3160.63	3159.0	3152.6	2999.6	3452.00	3600.29	3650.36
25	994.69	999.05	1094.66	718.00	734.01	732.12	740.55	682.45	702.59	765.79	766.28	754.55

B

Glucose (mM)	Glibenclamide			Nelf+Glibn			Saq+Glibn			Ata+Glibn		
11	6685.0	6714.00	6710.00	5571.19	5588.96	5616.94	5741.05	5770.80	5721.64	5411.14	5483.43	5381.401
15	8250.00	8189.00	8231.00	7195.27	7006.04	7370.71	6875.79	7270.28	7264.55	5869.82	6954.81	6765.519
20	8031.00	7961.00	7750.00	5494.08	5388.11	5500.36	5652.24	5640.90	5335.85	6064.94	6119.64	6203.210
25	8582.41	8614.14	8602.63	5114.94	5244.05	5172.80	4999.40	5067.84	5201.26	5275.23	5299.27	5281.660

Caspase -3 assay

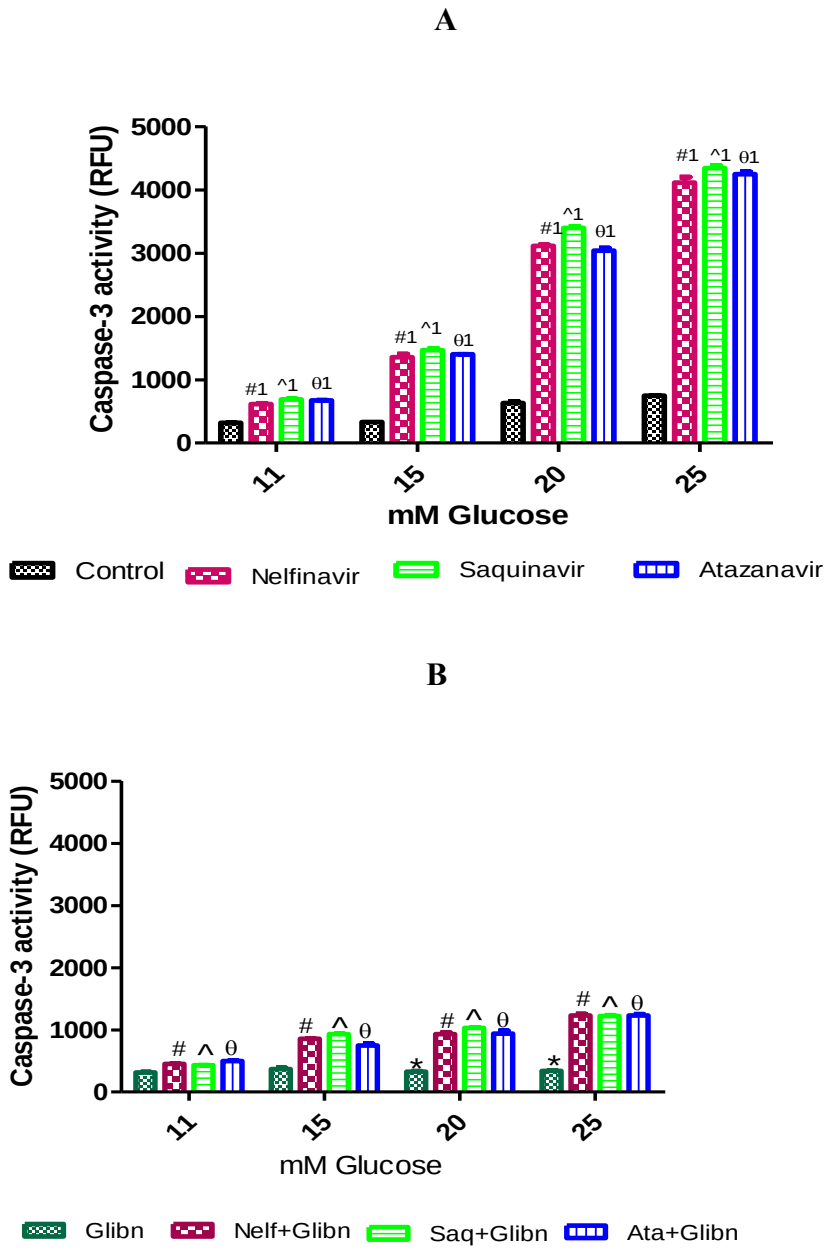

Figure 1: Caspase -3 activities in RIN-5F cells treated with PIs and glibenclamide (A/B) s for 24 h at 11-15 mM glucose concentration

A

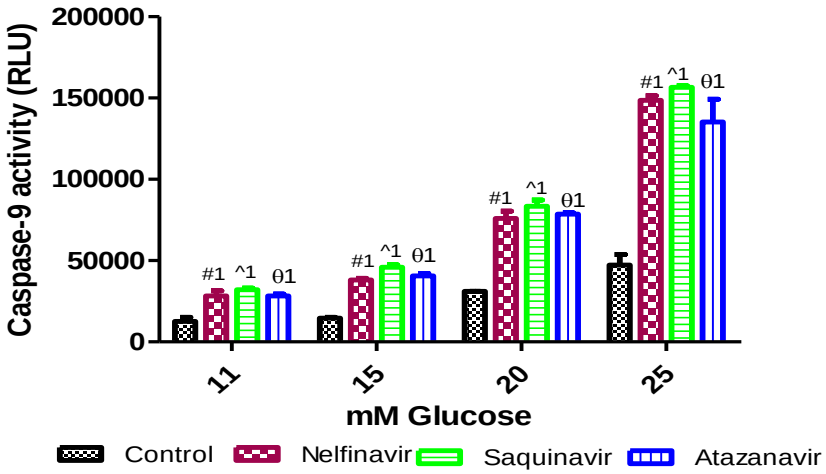

B

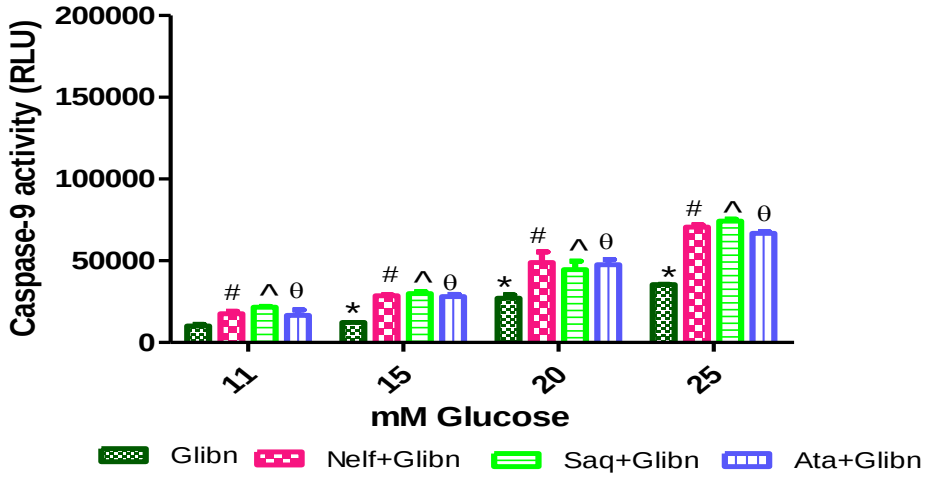

Figure 2: Caspase -9 activities in RIN-5F cells treated with PIs and/ glibenclamide (A/B) for 24 h at 11-15 mM glucose concentration

Table1: A dose-dependent increase insulin secretion in cells after naringin treatment for 24 h at 11 mM glucose.

Naringin (μM)	Insulin levels (μg/L)
0.0	1.0670
10.0	1.1845
20.0	1.6220
30.0	1.6920
40.0	1.9180
50.0	2.0905

Table 2: Malondialdehyde (lipid peroxidation) levels in RIN-5F cells treated with PIs and/ or naringin for 24 h at mM glucose concentration.

Control	**Nelfinavir**	**Saquinavir**	**Atazanavir**	**Naringin**	**Narg+Nelf**	**Narg+Saq**	**Narg+Ataz**
0.025	0.2780	0.358	0.275	0.041	0.040	0.037	0.041
0.023	0.3800	0.373	0.260	0.035	0.035	0.038	0.035
0.023	0.3780	0.283	0.260	0.038	0.036	0.036	0.037

Table 3: SOD activity after cells were exposed to PIs and/ or naringin for 24 hours at 11mM glucose concentration.

Control	Nelfinavir	Saquinavir	Atazanavir	Naringin	Narg+Nelf	Narg+Saq	Narg+Ataz
0.048	0.115	0.158	0.108	0.039	0.042	0.037	0.043
0.040	0.109	0.130	0.112	0.037	0.043	0.039	0.046
0.056	0.110	0.128	0.100	0.034	0.043	0.039	0.043

Table 4: Glutathione levels after cells were exposed to PIs and/naringin for 24 hours at 11 mM glucose concentration.

Control	Nelfinavir	Saquinavir	Atazanavir	Naringin	Narg+Nelf	Narg+Saq	Narg+Ataz
9501.0000	1210.4540	1152.4510	1538.2310	8058.0250	6900.0090	6610.4440	7119.3200
9616.1200	1281.5970	1071.1640	1420.9210	7898.2500	7550.2310	6400.2450	8125.4710
8896.3600	1381.9940	1159.6400	1454.5580	7601.0120	7380.1480	6820.0010	7080.1520

Table 5: ATP levels after cells were exposed to PIs and/ or naringin for 24 h at 11 Mm glucose concentration.

Control	Nelfinavir	Saquinavir	Atazanavir	Naringin	Narg+Nelf	Narg+Saq	Narg+Ataz
162.212	40.025	47.661	49.570	210.011	189.946	168.031	154.950
166.030	37.924	26.469	47.852	219.890	175.258	158.010	163.240
156.483	39.261	41.170	42.125	205.001	165.409	167.063	162.000

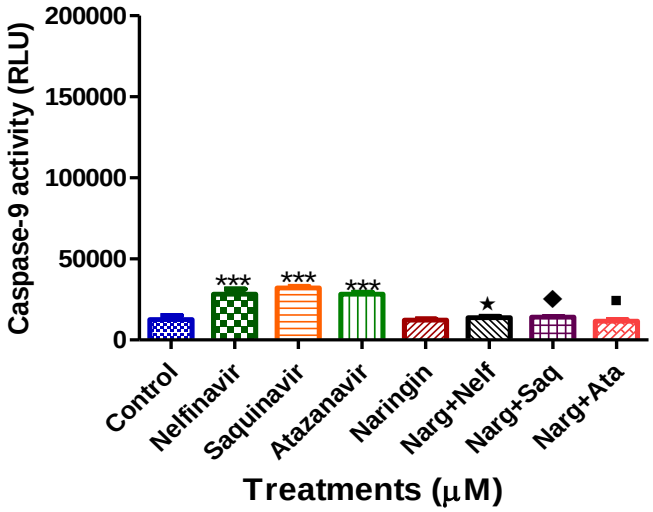

Figure 3: Caspase-9 activities in RIN-5F cells treated with PIs and naringin for 24 h at 11 mM glucose concentration.

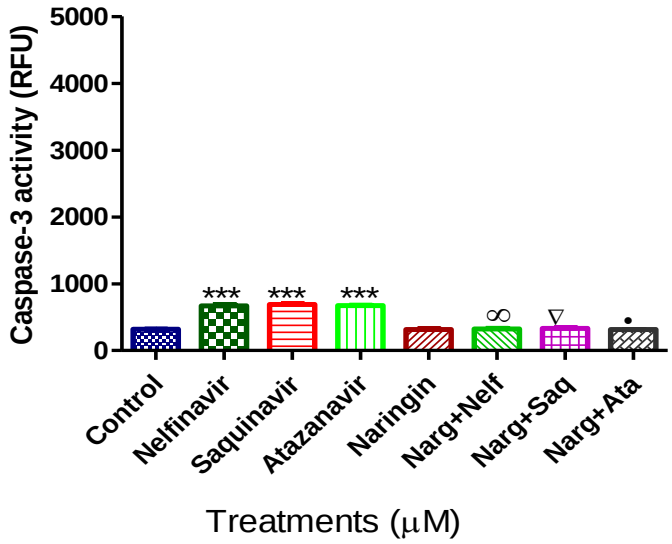

Figure 4: Caspase-3 activities in RIN-5F cells treated with PIs and naringin for 24 h at 11 mM glucose concentration.